TÉCNICO LISBOA

Optimal Scheduling of Demand-Responsive Services from Electric Vehicles in Distribution Grids

Pedro Miguel Santos Chaves

Thesis to obtain the Master of Science Degree in

Electrical and Computer Engineering

Supervisors: Prof. Hugo Gabriel Valente Morais
Prof. Pedro Manuel Santos de Carvalho

Examination Committee

Chairperson: Prof. Célia Maria Santos Cardoso de Jesus
Supervisor: Prof. Hugo Gabriel Valente Morais
Member of the Committee: Prof. António Manuel Raminhos Cordeiro Grilo

June 2024

Declaration

I declare that this document is an original work of my own authorship and that it fulfills all the requirements of the Code of Conduct and Good Practices of the Universidade de Lisboa.

Acknowledgments

As I reach the end of my academic journey, I look back with pride and joy to all the memories that I have made over the years. With this feeling of accomplishment, I want to thank everybody that made this possible.

First, I would like to express my deepest gratitude to my supervisors, Hugo Morais and Pedro Carvalho, for their invaluable guidance, support, and mentorship throughout this journey. Their expertise and constructive feedback have been instrumental in shaping this thesis and fostering my academic and professional growth.

I am profoundly grateful to my parents for their belief and encouragement, but most of all, for the love that they have always showed me. Their sacrifices and support have been the cornerstone of my success, and I am forever grateful to them. I extend my gratitude to my brother Bruno, who is always there for me when I need him, and has been a mentor and a companion in my journey. I always had his guidance and I now know that I always will.

I want to show my heartfelt appreciation to my colleagues and friends for their camaraderie, collaboration, and friendship throughout my academic experience and made this journey immensely rewarding.

I want to give a special thanks to my girlfriend Iryna, whose love, support, and understanding have been a constant source of strength and inspiration. When the motivation and discipline was lacking, she was the one that made me believe in myself and for that I am forever grateful.

Finally, I would like to thank all those who have contributed to this thesis in ways big and small, directly or indirectly. All the experiences that I had on this path, shaped me to the person that I am today. As a new phase of my life begins, I take the knowledge and lessons I learned throughout these years to guide me towards new objectives and new challenges.

Abstract

As the integration of Electric Vehicles (EV) becomes increasingly prevalent, the optimization of grid operations becomes paramount. This thesis addresses the challenges and opportunities posed by the evolving energy landscape, focusing on the optimal scheduling and resource allocation in the point of view of the Distribution System Operator (DSO). Through mathematical modeling and algorithmic optimization with Mixed-Integer Non-Linear Programming (MINLP), this thesis analyzes two distinct approaches to the management of EVs considering both Unidirectional Vehicle-to-grid (V1G) and Vehicle-to-grid (V2G) capabilities. The first approach centers on the DSO's role in managing grid resources efficiently while considering the dynamic nature of renewable energies and EVs, showing some cost minimization through the use of V2G but increasing the computational time of the optimization compared to the V1G technology. In the second model, the focus shifts to the coordination between the DSO and multiple Electric Vehicle Aggregators (EVA), each with distinct objectives and constraints. This model provides a decentralized approach to the EV management problem with a significant reduction in its time of optimization, while guaranteeing grid stability and supplied demand. The use of an aggregator increases the flexibility of the DSO when it comes to handle increases in power demands, showing that the decentralization of resource management does not compromise the grid's functioning. In summary, this thesis contributes to the discourse on grid management strategies in the face of increasing EV penetration and integration with other resources such as renewable energies. The findings shed light on the complexities of energy management in modern and future grid systems and analyze optimal decision-making strategies for grid operators.

Keywords

Demand Response; Distribution Grid; Electric vehicle; Electric Vehicle Aggregators; Vehicle-to-Grid.

Resumo

À medida que a integração de veículos eléctricos se torna cada vez mais prevalente, a otimização das operações da rede torna-se fundamental. Esta tese aborda os desafios e oportunidades colocados pela evolução do panorama energético, centrando-se na programação e gestão de recursos do ponto de vista do operador do sistema de distribuição. Através de modelação matemática e otimização, esta tese analisa duas abordagens distintas à gestão de veículos eléctricos, considerando as capacidades V1G e V2G. A primeira abordagem centra-se no papel do operador do sistema de distribuição na gestão eficiente dos recursos da rede, considerando a natureza dinâmica das energias renováveis e dos veículos eléctricos, mostrando alguma minimização de custos através da utilização de V2G, mas aumentando o tempo computacional da otimização em comparação com a tecnologia V1G. No segundo modelo, o foco passa a ser a coordenação entre o operador da rede de distribuição e múltiplos agregadores de veículos eléctricos, cada um com objectivos e restrições distintas. Este modelo permite uma abordagem descentralizada do problema de gestão de veículos eléctricos com uma redução significativa do seu tempo de otimização, garantindo a estabilidade da rede. A utilização de um agregador aumenta a flexibilidade do operador da rede de distribuição para lidar com aumentos na procura de energia, mostrando que a descentralização da gestão de recursos não compromete o funcionamento da rede. Em suma, esta tese contribui para o discurso sobre estratégias de gestão da rede face à crescente penetração de veículos eléctricos. Os resultados realçam as complexidades da gestão de energia e analisam estratégias de tomada de decisão óptimas para os operadores de rede.

Palavras Chave

Agregadores de veículos eléctricos; Rede de distribuição; Resposta à procura; Veículo elétrico; Veículo para a rede.

Contents

1 Introduction **1**

1.1 Motivation . . . 3

1.2 Objectives and contributions . . . 3

1.3 Related projects and scientific outputs . . . 4

1.4 Outline . . . 4

2 Background **7**

2.1 Demand-response . . . 10

2.2 Unidirectional Vehicle-to-grid (V1G) and Vehicle-to-grid (V2G) - Smart Charging and Discharging . . . 11

2.2.1 Ancillary services . . . 12

2.2.2 Integration with Renewable Energies . . . 13

2.2.3 Charging cost minimization . . . 13

2.2.4 Battery Degradation . . . 13

3 Related Work **15**

3.1 Scheduling of V1G . . . 17

3.2 Scheduling of V2G . . . 19

3.3 Electric Vehicle Aggregators (EVA) . . . 21

4 Methodologies **23**

4.1 Models . . . 25

4.1.1 Model 1: Electric Vehicles (EV)s managed by Distribution System Operator (DSO) 25

4.1.2 Model 2: Coordinated DSO/EVA control of EVs . . . 25

4.2 Mathematical Formulation . . . 26

4.2.1 Objective Functions . . . 27

4.2.2 Constraints . . . 29

4.2.3 Optimization . . . 36

5 Case study **39**
5.1 Distribution Network 41
5.2 Electric vehicle data 45
5.3 Electric vehicle aggregators data 46
6 Results **51**
6.1 Model 1: EVs managed by DSO 53
6.1.1 V1G solution 53
6.1.2 V2G solution 55
6.2 Model 2: Coordinated DSO/EVA control of EVs 59
7 Conclusion **69**
Bibliography **73**
A Distribution network data **81**
B Detailed results from the simulations **87**

List of Figures

2.1 Annual vehicle market share by fuel in Europe . . . 9
2.2 Demonstration of how a Demand Response (DR) program works . . . 10
2.3 Load levelling mechanism . . . 12

3.1 Relationship between droop control coefficient and SOC of the battery . . . 21

5.1 Distribution network used. . . . 41
5.2 Profile of the power generated by PV panels. . . . 43
5.3 Power demand profile. . . . 44
5.4 EV trip power consumption. . . . 46
5.5 Distribution of the busses per EVA. . . . 47
5.6 Distribution of EVs by EVAs (500 EVs). . . . 48
5.7 EVs driving pattern of each EVA. . . . 48
5.8 Opportunity cost curve. . . . 49
5.9 Cost of the power supplied by the DSO to the EVAs. . . . 50

6.1 Power scheduling for Model 1 considering only V1G . . . 53
6.2 Storage scheduling for Model 1 considering only V1G . . . 54
6.3 EVs scheduling for Model 1 considering only V1G . . . 55
6.4 Power scheduling for Model 1 considering V2G . . . 56
6.5 Storage scheduling for Model 1 considering V2G . . . 57
6.6 EVs scheduling for Model 1 considering V2G . . . 58
6.7 Voltage magnitude on every bus at period 20 . . . 59
6.8 EV charge profile on the first EVA scheduling . . . 60
6.9 EVA flexibility used throughout the days simulated by the DSO . . . 61
6.10 Evolution of the opportunity cost throughout the 10 days simulated . . . 61
6.11 Power scheduling by the DSO for days 1-4 . . . 62
6.12 EV charging and discharging schedule by EVA 1 for day 1 . . . 63

6.13 EV charging and discharging schedule by EVA 4 for day 1 64
6.14 EV charging and discharging schedule by EVA 2 for day 2 65
6.15 EV charging and discharging schedule by EVA 3 for day 2 65
6.16 Power scheduling by the DSO for days 8-10 66

List of Tables

4.1 Objective functions used for each model. 29
4.2 Constraints used for each model. 36

5.1 Number of Resources. 42
5.2 Characteristics of the generator types. 42
5.3 Quadratic cost of CHP generators. 43
5.4 Characteristics of the storage units. 44
5.5 Types of demand response programs. 45
5.6 Technical characteristics of the EVs considered. 45
5.7 DSO-EVA contract information. 49

6.1 Comparison of cost and time of optimizations 58
6.2 Optimization cost and power demand predicted by the EVAs 60
6.3 Optimization cost for the DSO and EVAs throughout the days (in m.u.) 66
6.4 Average time of optimization in Model 2 67

A.1 Base Values used for Per Unit system 82
A.2 Branches information 82
A.3 Load demand from period 1 to 7 83
A.4 Load demand from period 8 to 14 84
A.5 Load demand from period 15 to 21 85
A.6 Load demand from period 22 to 24 86

B.1 Model 1 results considering V1G from period 1 to 8 88
B.2 Model 1 results considering V1G from period 9 to 16 88
B.3 Model 1 results considering V1G from period 17 to 24 88
B.4 Model 1 results considering V2G from period 1 to 8 89
B.5 Model 1 results considering V2G from period 9 to 16 89

B.6 Model 1 results considering V2G from period 17 to 24 89
B.7 Model 2 results for day 1-4 from period 1 to 8 90
B.8 Model 2 results for day 1-4 from period 9 to 16 90
B.9 Model 2 results for day 1-4 from period 17 to 24 90
B.10 Model 2 results for day 8-10 from period 1 to 8 91
B.11 Model 2 results for day 8-10 from period 9 to 16 91
B.12 Model 2 results for day 8-10 from period 17 to 24 91

Acronyms

AEP	Average Electricity Price
AS	Ancillary Services
CHP	Combined Heat and Power
DER	Distributed Energy Resources
DG	Distributed Generation
DR	Demand Response
DSO	Distribution System Operator
EV	Electric Vehicles
EVA	Electric Vehicle Aggregators
EVeSSi	Electric Vehicle Scenario Simulator
GAMS	Generic Algebraic Modelling System
ICE	Internal Combustion Engine
HV	High Voltage
LV	Low Voltage
MATLAB	Matrix Laboratory
MILP	Mixed-Integer Linear Programming
MINLP	Mixed-Integer Non-Linear Programming
NLP	Non-Linear Programming
MV	Medium Voltage
PSO	Particle Swarm Optimization
PV	Photovoltaic
RCC	Rain-flow Cycle Counting

SOC	State of Charge
SR	Spinning Reserve
ToU	Time-of-Use
V1G	Unidirectional Vehicle-to-grid
V2G	Vehicle-to-grid

1

Introduction

Contents

1.1 Motivation 3
1.2 Objectives and contributions 3
1.3 Related projects and scientific outputs 4
1.4 Outline 4

This chapter dives into what motivated the development of this thesis, as well as what their objectives and contributions are set to. It also includes an outline of the structure of the thesis.

1.1 Motivation

The relentless degradation of our planet, motivated by the mass consumption of fossil fuels [1], has lead to a rise in the adoption of renewable energy sources and alternative energy technologies. As one of the primary contributors to environmental harm, the transportation sector is undergoing a profound transformation, with Electric Vehicles (EV) emerging as a promising solution. A recent study conducted by Eurelectric [2] forecasts a dramatic increase in EV adoption, with projections suggesting that by 2030, Europe alone will boast a staggering fleet of 65 million EVs, which means that it will increase forty times in 10 years. Similarly, within the Portuguese context, the study anticipates a substantial uptake, estimating approximately 655 thousand EVs [2] on the roads by the same year.

This impressive rise in EV adoption holds the promise of cleaner transportation, but it also presents an important challenge for the power grid. The substantial increase in electricity consumption, driven by the increase of EVs, is bound to pressure the grid infrastructure, leading to heightened power losses, voltage instability, peak power demands, and grid congestion [3]. To mitigate these challenges and ensure the seamless integration of EVs into the energy ecosystem, it is imperative to implement intelligent charging and discharging strategies, encompassing both Unidirectional Vehicle-to-grid (V1G) and Vehicle-to-grid (V2G) services.

1.2 Objectives and contributions

The objectives of this thesis are designed to address the pressing challenges posed by the integration of EVs into distribution grids and to explore strategies for optimizing their interaction with renewable energy sources and demand response mechanisms.

The formulation and implementation of optimization models to enable intelligent scheduling of EV charging and discharging, with a focus on both V1G and V2G services, is the primary objective of the study conducted, with the goal of minimizing the impact of the increasing number of EVs. These models test different approaches to the problems mentioned, considering different entities and different ways to manage EVs.

To analyze these models, simulations were made with the help of programs like Matrix Laboratory (MATLAB) and Generic Algebraic Modelling System (GAMS). A distribution network with a substantial penetration of EVs, as well as renewable energy sources, storage and other demand response programs, was simulated to implement the models proposed and assess their effectiveness

This thesis has the following contributions on these topics:

- Identification of the problems caused by the mass increase of EVs
- Analysis of new solutions to manage charging and discharging of EVs.
- Proposal of methodologies involving different entities, such as a Distribution System Operator (DSO) and Electric Vehicle Aggregators (EVA), and concept of their interactions.
- Formulation of the mathematical objectives and constraints to be taken into account for the models
- Simulation of the test scenarios and consequent analysis of its results.

1.3 Related projects and scientific outputs

The work carried out as part of this dissertation was developed under the scope of the following research project(s):

- Horizon Europe EV4EU – Electric Vehicles Management for carbon neutrality in Europe project, funded by the European Union under grant agreement no. 101056765. Views and opinions expressed are however those of the authors only and do not necessarily reflect those of the European Union or CINEA. Neither the European Union nor the grating authority can be held responsible for them.

1.4 Outline

This document is structured as follows. The present chapter introduces the main motivation and contributions of this thesis, as well as its objectives.

Chapter 2 offers foundational knowledge on EVs, including concepts of V1G and V2G technologies, as well as Demand Response (DR) mechanisms in grid management. Additionally, it delves into the integration of EVs within distribution grids, highlighting challenges and opportunities in this domain.

Chapter 3 explores recent research on applications of V1G and V2G, analyzing the objectives functions and constraints used, and what type of factors are taken into account in their scheduling.

Chapter 4 proposes a set of models for the optimal scheduling of EV charging and discharging in distribution grids, and explains in detail what methodologies are used.

In Chapter 5, the distribution network utilized for EV integration is thoroughly explained, alongside a detailed description of resources and dataset employed in the study.

Chapter 6 presents the findings obtained from the models in the case studies. It entails an in-depth analysis of model performance, comparison of case study outcomes, and interpretation of results in terms of the integration of EVs.

Finally, Chapter 7 summarizes the key findings of the study, discusses their implications for grid management and policy, acknowledges the limitations encountered, and proposes further future research.

2

Background

Contents

2.1 Demand-response 10
2.2 V1G and V2G - Smart Charging and Discharging 11

With the intensification of the energy crisis, governments have given great importance to the development of EVs in order to achieve decarbonisation. In Europe, a commitment was set to ban the commercialization of Internal Combustion Engine (ICE) vehicles by 2035, with some countries, like Norway, setting the goal for 2025 [4]. To accomplish such goal, a set of incentives for EV owners are being provided. 26 of the 27 members of European Union already offer these benefits, such as exemption of taxes and bonuses going all the way up to 10 000EUR per single EV, in the case of Romania [5].

Although representing just 9% of the total 326 million vehicle in Europe as of 2019, shown in Figure 2.1, these factors have already increased the EV share in the market to approximately 37% in just 2 years and it will contribute to a further growth, expecting 65 million vehicles by 2030 and double to 130 million vehicles by 2035 [2].

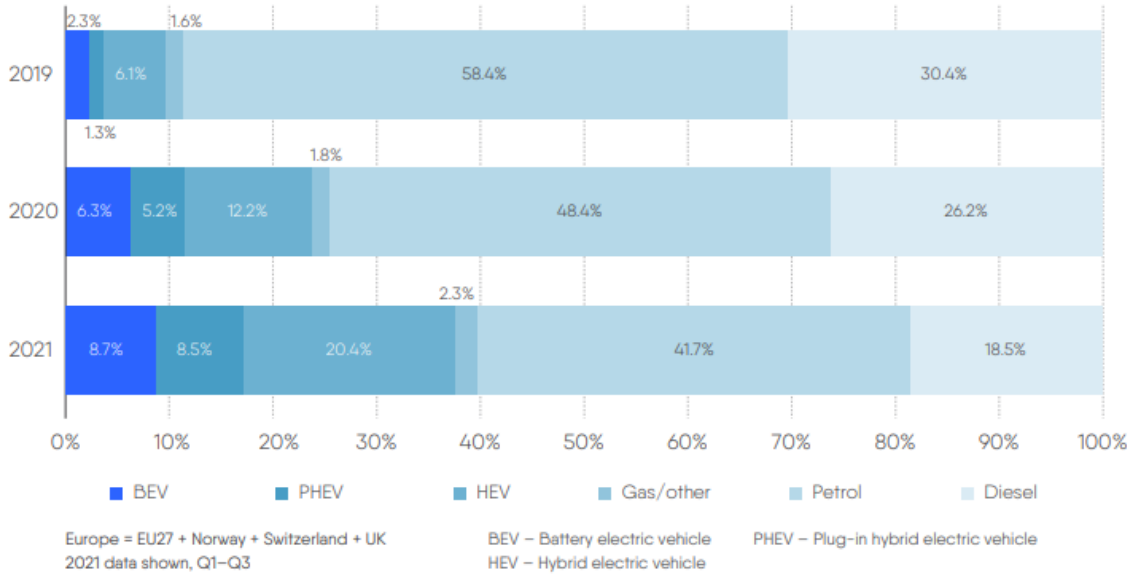

Figure 2.1: Annual vehicle market share by fuel in Europe [2]

The load profile of the electric system will be changed due to this mass adoption of EVs, resulting in the accelerated growth of 11% per year in the transport sector, adding 200 TWh to the demand by 2030 [2]. This will mean that approximately 5% of total demand in Europe will be from EVs, and by 2050, that number will increase to 9.5% [6].

When the number of EVs connected to the grid grows bigger, there may be a 'peak plus peak' phenomenon, meaning peak power load time coinciding with the peak EV charging time, increasing the amount of peaking power, grid construction pressure and reducing network operation efficiency, affecting the power grid safe and stable operation [7]. But the unpredictable nature of EV loads, could also disrupt the operations of the power systems. This unpredictability comes mainly from its high randomness in charging behavior. Random and uncontrolled charging could create problems for the

local grid and power quality, resulting in fast and unpredictable increases in demand that could lead to fluctuations in voltage, and power losses. Those variations will also impact the energy prices. Several strategies have been proposed and deeply studied, including demand-response mechanisms, smart charging and discharging protocols, and the provision of ancillary services. Additionally, integrating EVs with renewable energy sources and focusing on charging cost minimization are crucial for optimizing grid performance and stability. Moreover, understanding and mitigating battery degradation is essential for maintaining the long-term viability of EVs. The following sub chapters will delve into each of these areas, exploring their significance and the role they play in the integration of EVs into the power grid.

2.1 Demand-response

DR refers to alterations in the electricity consumption habits of end-users, deviating from their typical usage patterns in response to fluctuations in electricity prices or grid conditions [8]. DR encompasses all deliberate adjustments made by end-users to their electricity consumption patterns, with the goal of modifying the timing, intensity, or overall volume of electricity usage [9], as demonstrated in Figure 2.2.

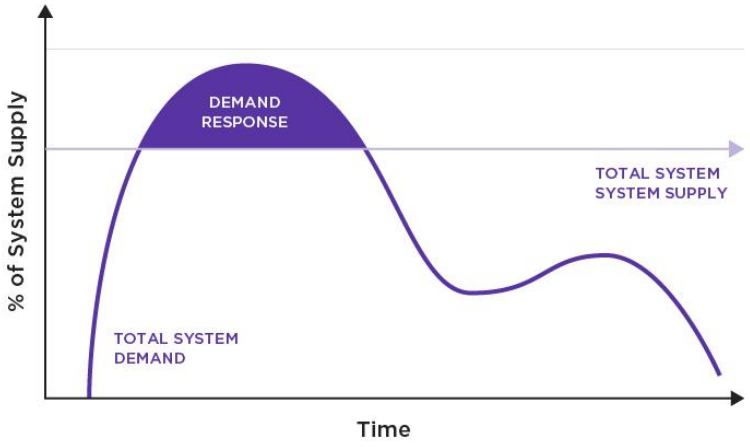

Figure 2.2: Demonstration of how a DR program works [10].

It provides benefits to its participants by offering incentives to modify their electricity usage patterns, leading to bill savings.

At a grid-wide level, DR initiatives contribute to price reduction by alleviating strain on the grid during peak demand periods. This increased capacity helps avoiding costly infrastructure upgrades, leading to reduced operational costs for utilities and potential savings for consumers, promoting cost efficiency

and sustainable grid development [11]. Moreover, DR programs have a positive impact on market performance by fostering a more competitive market environment [11]. By diversifying available resources and empowering consumers to participate actively in electricity markets, DR mitigates market power and promotes fair pricing.

DR programs can be divided into two types: incentive-based programs and price-based programs [12].

Incentive-based programs provide users with monetary incentives separate from electricity prices. These programs can encompass direct load control, where the operator has direct access to certain energy loads [13], interruptable/curtailable loads, where the consumer agrees to cut some of their load in critical situations [14], demand biding and buyback for larger consumers that curtail their demand at a bid price [15] and emergency demand reduction [16].

Price-based programs use smart-pricing to induce users to change their energy usage patterns. By having different electricity prices at different periods, consumers are more likely to alter their energy demands to save costs. These programs include Time-of-Use (ToU) pricing, [17], critical peak pricing [18] and real-time pricing (dynamic pricing), which is considered the most effective one [19].

DR initiatives typically target residential areas rather than commercial and industrial sectors, due to their higher sensitivity to fluctuations in electricity prices. This heightened sensitivity is attributed to the presence of a wider array of appliances that can be adjusted or controlled in response to price signals. The charging of EVs is a perfect example of that.

2.2 V1G and V2G - Smart Charging and Discharging

In normal charging, the EV starts to charge the moment it is plugged in at a constant rate. On the other hand, smart charging allows EV charging to be intelligently controlled, so it takes place when the electricity network has surplus capacity, or when there is reduced demand and electricity is cheaper. This process is denominated V1G. By controlling the charging power and the charging period of the day, grid congestion can be prevented. The power with which EV charge can be controlled remotely, so that the grid will be unburdened, resulting in peak shaving of the load profile.

An EV can also provide energy to the power grid by discharging the battery, a process which is known as V2G. Since most EVs are parked for long stretches of time [20], they can effectively perform both roles. Using intelligent scheduling of V2G means reshaping the load profile by charging the EV battery from the grid at the time when the demand is low and discharging the EV battery to the grid during peak hours [21].

V2G technology helps to boost the efficiency, reliability and stability of the grid through flexibility services such as load balancing, peak shaving, regulation of frequency and the support for the incorporation

of renewable energy [7].

2.2.1 Ancillary services

EVs can contribute to Ancillary Services (AS) in power systems, the main ones considered being frequency regulation, Spinning Reserve (SR) and load levelling [22].

Maintaining the power system frequency throughout the system is critically important. When the system frequency changes from it's normal value past the allowance tolerance, the generators in the power system must increase or decrease spin in order to regulate the frequency [23]. In transmission systems, there are three processes in frequency regulation, ranked in a hierarchical order by primary, secondary and tertiary control. Considering the uncertainty of EV scheduling, they can aide the primary control to stabilize the frequency to a stationary value [23].

When a contingency occurs, the SR respond [24]. Since most EVs are parked and not being used during a considerable part of the day [17], the energy stored in EV batteries can be used as SR. Compared with conventional generators, which are slow for grid synchronization due to startup issues, EVs have a much faster response time [25], thus increasing the reliability of the SR.

Load leveling, is a strategy employed to mitigate fluctuations in electrical load over a given period of time [26]. This process is composed of both valley filling and peak shaving combined, in order to flatten the load profile curve. The EVs charge during off-peak demand periods to fill the valley of the curve, and discharge during times of high demand in order to feed power back to the grid and shave the peak of the load curve [27]

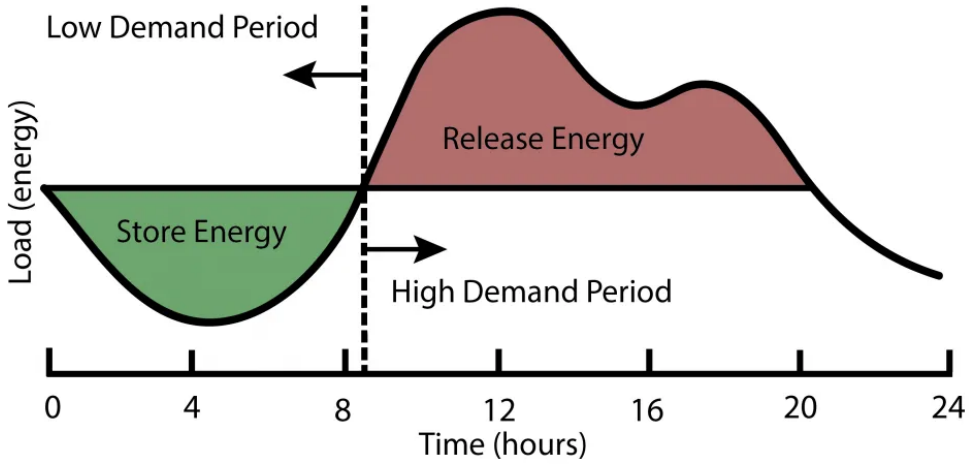

Figure 2.3: Load levelling mechanism [28].

The primary objective of load leveling is to balance the supply and demand of electricity by redis-

tributing loads across different time intervals, thereby reducing peak demand and ensuring more efficient utilization of resources within the electrical grid, such as renewables.

2.2.2 Integration with Renewable Energies

EVs have been suggested as one of the most promising solutions for mitigating the intermittent behavior renewable energy sources, such as wind and solar. As these sources depend heavily on the unpredictability of nature, their energy outputs greatly fluctuate throughout the day [29], which may lead to greater outputs during valley hours than during peak hours.

EVs can work as backup batteries, storing the excess energy from renewables that would otherwise be wasted. EVs owners can then use this stored energy for their daily driving routine,and can also supply this energy back to the network in times of high demand when the EV is not being used. This behaviour allows for bigger integration of renewables in the shares of electricity market, reducing its impact on the power systems [3].

2.2.3 Charging cost minimization

The ability to discharge energy back into the grid is not only favorable to the power systems, but also to the EV owners themselves. By charging the batteries at times when the energy price is lower, and discharging when the energy price increases, it generates revenue for the sale of energy back to the grid [30]. This results in a significant charging cost reduction to the owners, hence encouraging even more the adoption of EVs. [31] estimated that cash benefits due to V2G participation ranged from $392 to $561 annually for an individual EV owner charging at home only.

However, it should also be considered that the use V2G does come with additional costs such as expenses of required equipment, advanced communications and smart metering, and the faster degradation of batteries [3].

2.2.4 Battery Degradation

Battery efficiency and lifespan is one of the biggest challenges of the EV industry, considering that, in most cases, the battery accounts for more than 50% of the total vehicle cost [21].

Batteries have a limited amount of cycles, at the end of which they must replaced [32]. Many factors influence this number, such as depth of discharge, discharge rate, ambient temperature, charging regime and battery maintenance procedures [33]. Manufactures usually assume that the battery is fully charged and discharged each cycle at an ideal ambient temperature. But in V2G, the batteries are only partially discharged each cycle, going through more cycles on regular basis. This reduces their lifespan, meaning

that it will have to be replaced sooner than with normal uncontrolled charging, increasing the cost to the EV owner.

3

Related Work

Contents

3.1 Scheduling of V1G 17

3.2 Scheduling of V2G 19

3.3 EVA 21

This chapter explores the existing literature in the field, offering an extensive review of key studies, theoretical frameworks, and empirical research. Following this, it delves into the mathematical formulations, objective functions, and constraints employed by researchers in addressing the scheduling of resources in a grid context.

EV charging modeling involves factors such as EV battery properties, types of EV, travel time, mileage, charging properties and charging time. The existing work on the scheduling of demand responsive services for EVs can be classified into two classes:

- Considering charging only (V1G).
- Considering charging and discharging (V2G).

3.1 Scheduling of V1G

In V1G, the scheduler tries to optimize the energy flow from the grid to the battery of the EV.

The authors of [34] consider a specific scenario for 55 distribution networks in The Netherlands, combining recent and future EV load profiles, concluding that controlled charging results in a significant reduction of overloaded network components compared to the uncontrolled charging, specially in the High Voltage (HV)/Medium Voltage (MV) transformer station level, followed by MV/Low Voltage (LV) transformers and MV cables.

In [35], orderly charging strategy is proposed using a multi-objective optimization model with a minimum peak-to-valley difference and minimum charging cost, setting as constraints the load limit, the EV charging time and the user demand, resulting in following objective function F:

$$min(F) = (\sum_{i=1}^{N_{EV}} \sum_{t=1}^{T} \lambda_t * P_{ev} * X_{i,t} * \Delta t) \tag{3.1}$$

, where T represents the number of optimized time periods and t represents the number of the optimization period; λ_j represents the time-sharing charging price of period t; P_{ev} represents the charging power of the EV; $X_{i,j}$ is a binary that represents the charging state of the i-th electric vehicle in period t; Δt represents the optimization interval; N_{EV} represents the total number of EVs considered. The electric vehicle load power and electricity consumption is calculated with Monte Carlo simulation, considering daily arrival time and daily mileage probability distribution, using a normal distribution for the arrival time:

$$f_{arrival}(t) = \frac{1}{\sigma\sqrt{2\pi}} exp[-\frac{(t-\mu)^2}{2\sigma^2}] \tag{3.2}$$

and a lognormal distribution for the daily mileage:

$$f_{mileage}(x) = \frac{1}{x}\frac{1}{\sigma\sqrt{2\pi}}exp[-\frac{(lnx-\mu)^2}{2\sigma^2}] \tag{3.3}$$

This model is then solved using weighted minimum modulus ideal point method, a method based on the Particle Swarm Optimization (PSO), that is also used in [36].

In [37], a normal probability distribution is used to estimate the time of arrival and departure of EV based on surveys of American vehicle users, a similar distribution to the one used in [35], but it does not consider the daily mileage of each EV, assuming that each EV takes the same time to finish charging.

Although the models shown in [37] and [35] show that smart charging has great benefits for cost minimization, they do not consider other uses for EVs, such as storage for renewables.

In [38], a stochastic model of EVs charging loads is developed to analyze its impact on distribution power grid considering two types of vehicles: public transportation and private vehicles. Then, output data of a wind power/battery energy storage system and real-time pricing was used as to make better use of surplus wind power and save money on EV charging cost. As it is a stochastic model, it considers the uncertainties and randomness of the energy price and power output, as well as the number of EVs plugged in.

In [39], three types of charging patterns are considered, each one with different distribution probabilities of charging time throughout the day, but only the charging time pattern coinciding the peak load is optimized, as it is the most problematic for the grid.

In [40], a dynamic multi-objective selection mechanism based on the power supply margin of distribution transformers is proposed to control the charging power of electric vehicles and initial charging time. For this, six optimization objectives are set, each one with its own objective function, regarding load peak, peak valley load difference, load fluctuation, sum of voltage offset in each node, power grid losses and charging cost. The constraints used are the EVs battery charging capacity and the limits the system power flow, the voltage amplitude and the line capacity. To optimize the model, a selection factor $\varphi(t)$ is used:

$$\varphi(t) = (1 - \frac{P_i(t)}{\eta_T * C_T})\% \tag{3.4}$$

where $P_i(t)$ is the load power in node i at instant t and η_T and C_T are the efficiency and capacity of the distribution transformer, respectively. This factor chooses which optimization goals are considered at any given time according to thresholds set. The optimization goals are then solved using the same method as [35] and [36].

Even though V1G research shows great results regarding cost minimization for EV users and peak-shaving the load profile for the distribution grids, as well as better use of renewable energies in power distribution, V2G might be another alternative that researchers have been studying deeply, to compre-

hend in what ways in can improve on the smart-charging mechanism.

3.2 Scheduling of V2G

In V2G, another level of complexity is added, with the scheduler trying not only to optimize the energy flow from the grid to the battery of the EV but also from the EV to the grid. Further complexity can be added according to which goals are aimed to be optimized.

The authors of [30], [41] and [42] focus purely on the maximization of charging benefits for EV owners, considering similar constraints. In [30], a 14 node distribution grid is simulated. Taking into account several constraints related to electricity price, battery capacity and state of charge, the objective of maximizing the benefits by charging the EV batteries when the price is low and discharging when the price is high and is given as follows:

$$max(F) = \sum_{i=1}^{n}((\lambda_t - K)P_{disi}) - \sum_{i=1}^{n}(\lambda_t)P_{chi} \tag{3.5}$$

where P_{chi} and P_{disi} are the charging and discharging rate of each EV, respectively, and K is a constant used to prevent the simultaneous charging and discharging process of the batteries. Setting an Average Electricity Price (AEP) and with State of Charge (SOC) of the vehicle, the algorithm proposed is able differentiate between 5 available modes, from charging, discharging, stand-by for both the previous cases and finally, when the EV is not available, meaning it is not at a charging station. In [41], a day-ahead scheduling strategy for a fleet of EVs plugged-in to the grid is studied, which is then optimized using a deterministic linear programming formulation. The optimisation objective function used is similar to Equation (3.1), also proposed by [35], but as it is implemented for V2G use, it allows negative power, representing the discharging of the EV to the grid. The algorithm is applied in a simulated industrial microgrid.

Both [42] and [43] consider battery degradation on the scheduling. [42] also uses a linear programming model, while considering the battery degradation costs, formulating the objective function shown in Equation (3.6) to minimize total costs for EV owners. The costs for battery degradation are modeled by a quadratic function.

$$min(F) = \sum_{i=1}^{T} X_t[(\eta_{dis}P_{dis}\gamma_t)y_t - (P_{ch}\lambda_t + (P_{ch}\eta_{ch})^2\lambda_p + P_{ch}\eta_{ch}\lambda_e)x_t] \tag{3.6}$$

X_t is a binary stating the availability of the vehicle; x_t and y_t are also binaries stating if it is charging or discharging; η_{ch} and η_{dis} represent the efficiencies of the charging and discharging processes; P_{ch} and P_{dis} are the charging and discharging powers; λ_t is the electricity price at instant t; γ_t is the electricity

price benefit for the EV at instant t; λ_p and λ_e represent the battery degradation cost associated with power and energy throughput respectively.

With the goal of minimizing battery degradation, [43] proposes a battery anti-aging V2G behavior management method, based on Rain-flow Cycle Counting (RCC) algorithm, where the minimal battery aging effect was set as one of the optimization objectives in a multi-objective optimization problem, represented by the function:

$$min(F) = \sum_{i=1}^{n} N_i^{cycle} + N_i^{hcycle} \tag{3.7}$$

where N_i^{cycle} and N_i^{hcycle} represent the number of full cycles and half cycles, respectively, of the EV battery in V2G. This anti-aging method aims to reduce the number of cycles and half cycles, thus increasing the lifespan of the batteries used in V2G applications.

In [44], the user convenience is set as one of the main objectives of the optimization problem. Despite bringing economic benefits for EV owners, it also impacts on user convenience of random travel, as the battery may not be sufficiently charged at some particular moment. To account for this, a virtual price λ_{inc}, that represents the inconvenience of V2G, is added to the optimization, which can be adjusted to the user's type of random travel demand.

The authors of [25], [45] and [46] take into account the AS that can be provided with V2G. In [25], the optimization of scheduling for both spinning reserve and user cost is studied, building a mathematical model to represent the spinning reserves taking into account EV mobility and adding a constraint to insure that it always meets the minimum requirement of spinning reserve power in the grid, but it does not take into account the peak-shaving capabilities of V2G.

$$P_{res}(t) \geq P_{res_{min}}(t) \tag{3.8}$$

In [45], a model to provide frequency regulation services is proposed, adding a regulation request parameter assuming that the regulation services are zero-energy services, meaning the expectation of the energy required for regulation services is zero over a very long time period. In [46], a V2G control strategy is studied to maintain the battery energy and provide frequency regulation done by droop control. When the frequency fluctuates above or below the set maximum frequency variation, additional power is discharged from the EV to the grid. That power is influenced by the regulation coefficients K_c and K_d, for charging and discharging respectively, depending on the SOC of the battery, as shown in Figure 3.1. Both [45] and [46] fail to consider user costs.

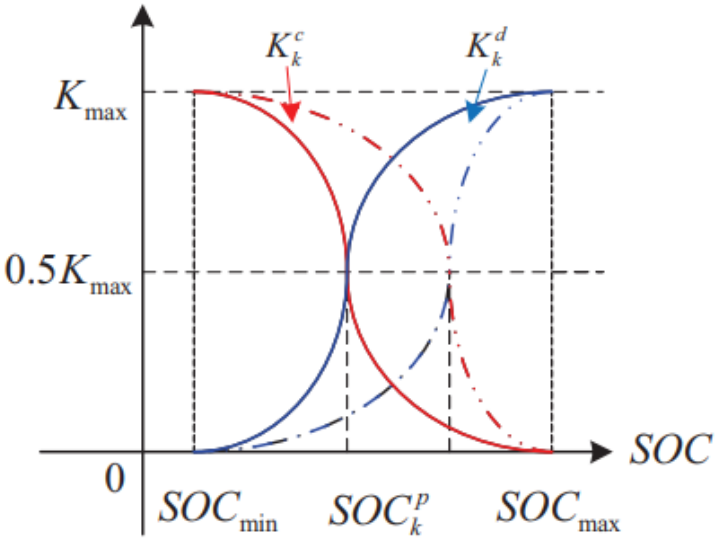

Figure 3.1: Relationship between droop control coefficient and SOC of the battery [46].

[47] proposes a mobility-aware V2G control algorithm where EVs can act as energy transporters among different microgrids to balance power demand between regions of high and low demand. This is done considering the mobility of EVs, states of charge of EVs, and the estimated/actual demands of microgrids, which is then optimized by a Markov decision process, a discrete-time stochastic control method.

3.3 EVA

On the topic of how the management of EVs is done, several studies propose the concept of EV fleet operators or EVA. The authors of [48] describe these entities as operators "that can exploit the flexibility potential of EVs, by participating in flexibility markets and by controlling both the time and the charging and discharging rate of connected EVs". The objective behind this aggregation is to decrease the cost of the operation and to represent the interests of the aggregated resources such as EVs in the electricity market. The presence of an aggregator in the energy market could increase the profit for each smaller scale producer or resource, when compared to the scenario in which each one individually negotiates with the grid operator.

The authors of [3] investigate the multifaceted roles of EVs within smart grids, focusing on how an EVA operates in conjunction with other types of operators at transmission and distribution levels in terms of control and communication. However, this study fails to achieve concrete numerical results of its benefits.

In [49] are considered scenarios with real data of market prices in a stochastic manner, taking into account uncertainties related to the EV owner's behavior, but also the comfort of the EV owners by

guarantying minimum desired charge levels. The study results show significant profit to the EVA while participating in the day ahead and reserve markets.

On a different approach, [50] studies the use of a cooperative gaming model with real-time electricity price, where the DSO, as the leader, regulates the load profiles, while an EVA, as the follower, schedules the EV charging and discharging behaviors according to the strategies of the grid operators. Both sides compete to improve the revenue and reduce the costs as much as possible, until reaching an equilibrium point.

All in all, the research suggests that the implementation of EVA can represent a critical component in the transition towards more sustainable and resilient grids with a high penetration of EVs, facilitating their integration.

4

Methodologies

Contents

4.1 Models 25
4.2 Mathematical Formulation 26

This chapter presents the proposed models for solving the optimal scheduling problem considering an intensive use of EVs, starting with a description of how the models work, followed by their mathematical formulation, namely the objective functions and constraints used, and finally an explanation on how the optimisation was accomplished.

4.1 Models

The advancement of power distribution systems has started a period characterized by new challenges. In this evolving landscape, the integration of Distributed Generation (DG), Distributed Energy Resources (DER), EVs, and energy storage play an important role, along with the integration of renewable energy sources, in maintaining reliability, optimizing resource allocation, and ensuring cost-effective operation. To address these challenges, different models of grid management have emerged. This thesis explores two distinct deterministic models: one where the DSO assumes comprehensive control over all grid resources, and another where the DSO collaborates with EV aggregators for more efficient management.

4.1.1 Model 1: EVs managed by DSO

In the first model, the DSO assumes comprehensive control over all grid resources, encompassing loads, generators, storage systems, and EVs. This centralized approach empowers the DSO to orchestrate and optimize the entire distribution network's operation, ensuring efficiency, stability, and reliability. Under this model, the DSO leverages data from consumers and control algorithms to balance supply and demand, manage voltage levels, and enhance grid resilience. Additionally, it can facilitate the integration of renewable energy sources, such as solar power, by coordinating their output and storage. Two types of demand response for the loads are also considered, the first with continuous regulation, meaning the DSO can reduce the load until a certain percentage, and the other with discrete regulation, where it can cut a fixed value of the load [51]. These programs are denominated reduce and cut DR, respectively.

This model will be studied considering both scenarios of EV capabilities, V1G and V2G, to analyze its impacts.

4.1.2 Model 2: Coordinated DSO/EVA control of EVs

In the second model, the DSO retains its role as the primary manager of grid resources, with the exception of EVs. In this scenario, EVs are managed by specialized entities known as EVA, which hold contracts with the DSO. These contracts are based on two critical factors: power and flexibility.

The EVA specifies a certain amount of power it requires from the grid on a daily basis. This power demand represents the minimum amount of electricity needed to meet the operational requirements of

its EV fleet. This demand is essential to ensure that the EVA can fulfill its commitments to its customers, such as charging EVs within specified time frames.

Beyond the fixed power demand, the EVA is granted a degree of flexibility in its power supply arrangements. Flexibility means that the EVA can receive less power than originally demanded, within predefined limits. This flexibility acknowledges the dynamic nature of grid operations and allows for adjustments in real-time. It provides the EVA with the capacity to adapt to unforeseen circumstances or grid constraints imposed by the DSO [52].

When the DSO fails to distribute the full power demand specified by the EVA but remains within the flexibility bounds, an opportunity cost is applied. This cost operates on a sliding scale, meaning that it starts at a relatively low cost and increases with every hour the DSO falls short of supplying the full power demand. When it reaches the max amount of hours of unsupplied demand, the opportunity cost reaches its maximum value. This cost is designed to incentivize the DSO to meet the EVA's power demands promptly, making use of the flexibility offered. If the EVA cannot supply the power demand, even within the granted flexibility, a penalty cost is imposed. This cost serves as a more severe penalty, reflecting a failure to meet contractual obligations when the flexibility available is not respected [53]. It provides a strong incentive for the DSO to ensure that power commitments to the EVA are met, even under challenging grid conditions. The two demand response programs will also be considered for this model, meaning the DSO will have the option of reducing and cutting certain loads at peak hours.

Unlike the previous model, the DSO + EVA model will only be simulated with V2G capabilities, as the main focus is to analyze the interaction between the DSO and the EVAs in terms of the use of the flexibility in power demanded provided by EVs. The ability of EVs to provide energy back to the grid will not alter significantly the use of their flexibility, as their charging and discharging will occur at different periods.

These two models present distinct approaches to grid management, with Model 1 emphasizing centralized control by the DSO and Model 2 introducing a specialized role for EVA in managing electric vehicle resources within the grid ecosystem.

4.2 Mathematical Formulation

To be able to simulate the models described, mathematical equations must be formulated to establish the relation between the different entities and resources. For this, objective functions must be set, as well as the constraints imposed.

4.2.1 Objective Functions

For the first model, the objective function ($F_{1_{DSO/V2G}}$) formulated represents the minimization of the operation cost of all aggregated resources by the DSO, and is defined as:

$$
\begin{aligned}
min(F_{1_{DSO/V2G}}) = \sum_{t=1}^{T}(\sum_{GEN=1}^{N_{GEN}} (\lambda_{A(GEN,t)} + \lambda_{B(GEN,t)} P_{GEN(GEN,t)} + \lambda_{C(GEN,t)} P^2_{GEN(GEN,t)}) + \\
\sum_{LOAD=1}^{N_{LOAD}} (\lambda_{LOAD_{Red}(LOAD,t)} P_{LOAD_{Red}(LOAD,t)} + \\
\lambda_{LOAD_{Cut}(LOAD,t)} P_{LOAD_{Cut}(LOAD,t)}) + \\
\sum_{EV=1}^{N_{EV}} ((\lambda_{EV_{dis}(EV,t)} + \lambda_{deg}) P_{EV_{dis}(EV,t)} + \lambda_{EV_{rx}(EV,t)} E_{EV_{rx}(EV,t)}) + \\
\sum_{ST=1}^{N_{ST}} \lambda_{ST_{dis}(ST,t)} P_{ST_{dis}(ST,t)} + \\
\sum_{GEN=1}^{N_{GEN}} \lambda_{GEN_{Exc}(GEN,t)} P_{GEN_{Exc}(GEN,t)} + \\
\sum_{LOAD=1}^{N_{LOAD}} \lambda_{LOAD_{Ens}(LOAD,t)} P_{LOAD_{Ens}(LOAD,t)})
\end{aligned}
\tag{4.1}
$$

The generators are expressed in a quadratic function where $P_{GEN(GEN,t)}$ represents the power generated by each generator and $\lambda_{A(GEN,t)}$, $\lambda_{B(GEN,t)}$ and $\lambda_{C(GEN,t)}$ are the coefficients used for their price. For the demand response of the loads, $P_{LOAD_{Red}(LOAD,t)}$ and $P_{LOAD_{Cut}(LOAD,t)}$ represent the power reduced and the power curtailed respectively, each one with their own price, represented by $\lambda_{LOAD_{Red}(LOAD,t)}$ and $\lambda_{LOAD_{Cut}(LOAD,t)}$. For EVs, $\lambda_{EV_{dis}(EV,t)}$ is used to represent the cost of discharging their batteries, followed by its respective power, $P_{EV_{dis}(EV,t)}$. The degradation cost of the batteries is represented with λ_{deg}. To deal with impossible requests from the EV users, a relaxation variable $E_{EV_{rx}(EV,t)}$ is used, associated with a high cost $\lambda_{EV_{rx}(EV,t)}$. This variable is only used when an EV demands a power that is impossible to supply in the period that the EV is connected. Similarly, the storage units are considered with $\lambda_{ST_{dis}(ST,t)}$ being their discharging price, and $P_{ST_{dis}(ST,t)}$ being their discharging power. It is important to note that the discharging of the EVs and storage units are considered expenses to the DSO, thus not appearing in the objective function.

The DSO also has the responsibility of using all the energy generated by the DG units, hence having to pay a cost for the excess power that is not dispatched, represented by $\lambda_{GEN_{Exc}(GEN,t)}$ and $P_{GEN_{Exc}(GEN,t)}$. Another cost, denoted as $\lambda_{LOAD_{Ens}(LOAD,t)}$, is used in situations where the DSO encounters insufficient generation capacity to fulfill the entire power consumption of consumers. This cost serves as a mechanism to mitigate non-supplied demand represented by $P_{LOAD_{Ens}(LOAD,t)}$.

Equation 4.1 refers to the objective function of the DSO model considering V2G, as it allows the discharge of EV's batteries into the grid. If only V1G is considered, then the objective function changes, with the only difference being the exclusion of the variables $\lambda_{EV_{dis}(EV,t)}$ and $P_{EV_{dis}(EV,t)}$, relating to the discharging of EVs.

For the DSO + EVA model, two objective functions will have to be considered, one for the DSO and other for the EVA.

Considering that the DSO no longer has the responsibility to manage EV's charging and discharging schedule, the variables related to them disappear from its objective function, being replaced with the variables specifying the contracts with the EVAs.

$$
\begin{aligned}
min(F_{2_{DSO}}) = \sum_{t=1}^{T}(& \sum_{GEN=1}^{N_{GEN}} (\lambda_{A(GEN,t)} + \lambda_{B(GEN,t)} P_{GEN(GEN,t)} + \lambda_{C(GEN,t)} P^2_{GEN(GEN,t)}) + \\
& \sum_{LOAD=1}^{N_{LOAD}} (\lambda_{LOAD_{Red}(LOAD,t)} P_{LOAD_{Red}(LOAD,t)} + \\
& \lambda_{LOAD_{Cut}(LOAD,t)} P_{LOAD_{Cut}(LOAD,t)}) + \\
& \sum_{EVA=1}^{N_{EVA}} (\lambda_{OP(EVA,t)} (P_{EVA_{ChCont}(EVA,t)} + P_{EVA_{dis}(EVA,t)}) + \\
& \lambda_{PEN(EVA,t)} P_{EVA_{ChNonCont}(EVA,t)}) + \\
& \sum_{ST=1}^{N_{ST}} \lambda_{ST_{dis}(ST,t)} P_{ST_{dis}(ST,t)} + \\
& \sum_{GEN=1}^{N_{GEN}} \lambda_{GEN_{Exc}(GEN,t)} P_{GEN_{Exc}(GEN,t)} + \\
& \sum_{LOAD=1}^{N_{LOAD}} \lambda_{LOAD_{Ens}(LOAD,t)} P_{LOAD_{Ens}(LOAD,t)})
\end{aligned}
\tag{4.2}
$$

As said contracts have two costs associated with them, $\lambda_{OP(EVA,t)}$ and $\lambda_{PEN(EVA,t)}$ are used to represent them, those being opportunity cost and penalty cost. The opportunity cost relates to the contracted power $P_{EVA_{ChCont}(EVA,t)}$, which is the power curtailment by the DSO, that respects the flexibility offered by the EVA. The penalty cost, on the other hand, relates to the non contracted power $P_{EVA_{ChNonCont}(EVA,t)}$, which is the unsupplied power that goes beyond the flexibility offered by the EVA.

The EVAs will also have to have an objective function, as they also intend to minimize costs. As they're only responsible for the scheduling of EVs, their objective function will only have terms related to the charging and discharging of EVs.

$$min(F_{2_{EVA}}) = \sum_{t=1}^{T} \sum_{EV=1}^{N_{EV}} ((\lambda_{EV_{dis}(EV,t)} + \lambda_{deg}) P_{EV_{dis}(EV,t)} + \lambda_{DSO_{supply}(t)} P_{EV_{ch}(EV,t)} + \lambda_{EV_{rx}(EV,t)} E_{EV_{rx}(EV,t)}) \tag{4.3}$$

The variable $\lambda_{DSO_{supply}(t)}$ represents the cost of the energy supplied by the DSO for the EV charging, as the EVAs do not have generation and must pay the DSO for the energy used. The opportunity and penalty costs are not taken into account in the objective function of the EVAs, as it is independent from the EVA choices.

Model	Used by	Objective functions
Model 1	DSO	4.1
Model 2	DSO	4.2
	EVA	4.3

Table 4.1: Objective functions used for each model.

4.2.2 Constraints

All the objective functions introduced previously have to submit to certain constraints to ensure that power and energy limits are not exceeded, as well as the proper functioning of the grid.

Starting with the DG units, the generators have to obey limits of maximum and minimum power. The external suppliers and Combined Heat and Power (CHP) units obey the following constraints:

$$P_{GEN(GEN,t)} \leq P_{GEN_{max}(GEN,t)} \tag{4.4}$$

$$P_{GEN(GEN,t)} > P_{GEN_{min}(GEN,t)} \tag{4.5}$$

Photovoltaic (PV) units units have a fixed power generation constraint, meaning the active power generated will always have to be equal to the maximum allowed.

$$P_{GEN(GEN,t)} = P_{GEN_{max}(GEN,t)} \tag{4.6}$$

As for reactive power $Q_{GEN(GEN,t)}$, it is also subject to an upper limit.

$$Q_{GEN(GEN,t)} < Q_{GEN_{max}(GEN,t)} \tag{4.7}$$

Regarding the loads, the power that can be cut or reduced is subject to a maximum value.

$$P_{LOAD_{Red}(LOAD,t)} < P_{LOAD_{Red_{max}}(GEN,t)} \tag{4.8}$$

$$P_{LOAD_{Cut}(LOAD,t)} = P_{LOAD_{Cut_{max}}(LOAD,t)} X_{LOAD_{Cut}(LOAD,t)} \tag{4.9}$$

$X_{LOAD_{Cut}(LOAD,t)}$ represents a binary variable, as the power can either be curtailed, or not. Also a constraint is added to be able calculate the amount of reactive power that the loads consume, $Q_{LOAD(LOAD,t)}$, based on the power that is actually supplied to each load and the power angle $\phi(LOAD, t)$

$$\begin{aligned} Q_{LOAD(LOAD,t)} = (P_{LOAD(LOAD,t)} - P_{LOAD_{Cut}(LOAD,t)} - \\ P_{LOAD_{Red}(LOAD,t)} - P_{LOAD_{Ens}(LOAD,t)}) * \tan\phi(LOAD, t) \end{aligned} \tag{4.10}$$

For the storage units, the charging and discharging power rates are subject to an upper bound, as demonstrated in :

$$P_{ST_{Ch}(ST,t)} \leq P_{ST_{Ch_{max}}(ST,t)} X_{ST_{ch}(ST,t)} \tag{4.11}$$

and

$$P_{ST_{Dis}(ST,t)} \leq P_{ST_{Dis_{max}}(ST,t)} X_{ST_{dis}(ST,t)} \tag{4.12}$$

where $X_{ST_{ch}(ST,t)}$ and $X_{ST_{dis}(ST,t)}$ represent binary variables to show if the storage unit is either charging or discharging. As they cannot be simultaneously charging and discharging, a constraint is introduced to demonstrate this using those binary variables.

$$X_{ST_{ch}(ST,t)} + X_{ST_{dis}(ST,t)} \leq 1 \tag{4.13}$$

As batteries have a limited capacity, the amount of energy in them that the model will consider will also have to be limited.

$$E_{ST(ST,t)} \leq E_{ST_{max}(ST,t)} \tag{4.14}$$

To avoid battery damage, a minimum amount of energy is also set in the storage units.

$$E_{ST(ST,t)} \geq E_{ST_{min}(ST,t)} \tag{4.15}$$

With this limited capacity in mind, the storage unit cannot charge or discharge indefinitely between two time steps, so it is necessary to have constraints that relate the previous SOC to the current ones,

hence

$$E_{ST(ST,t)} = E_{ST(ST,t-1)} + \eta_{ST_{ch}} * P_{ST_{ch}(ST,t)}\Delta t - (1/\eta_{ST_{dis}}) * P_{ST_{dis}(ST,t)}\Delta t \tag{4.16}$$

where $\eta_{ST_{ch}}$ and $\eta_{ST_{dis}}$ represent the charging and discharging efficiencies of the storage units, respectively.

From this, two new constraints take shape, one to prevent the batteries from overcharging.

$$\eta_{ST_{ch}} P_{ST_{ch}(ST,t)}\Delta t < E_{ST_{max}(ST,t)} - E_{ST(ST,t)} \tag{4.17}$$

and another to prevent them from over-discharging

$$(1/\eta_{ST_{dis}}) P_{ST_{dis}(ST,t)}\Delta t < E_{ST(ST,t-1)} \tag{4.18}$$

Δt represents the time step used in the optimisation.

Finally, the storage units are set to have a certain amount of energy stored for the next day.

$$E_{ST(ST,24)} \geq E_{ST_{min_{final}(ST)}} \tag{4.19}$$

Equation 4.19 guarantees that at the final period of the day, the storage have energy to accommodate the next day scheduling, with $E_{ST_{min_{final}(ST)}}$ representing the final value of energy that needs to be stored. Similarly to the storage units, the EVs work as batteries, therefore needing constraints to limit battery capacity as seen in Equation 4.20.

$$E_{EV(EV,t)} < E_{EV_{max}(EV,t)} \tag{4.20}$$

The EV batteries need to always keep a certain amount of minimum energy, to avoid damage to the lifespan of the battery [54], but mainly to accommodate for the need of the user for the next trip, considering the relaxation variable $E_{EV_{rx}(EV,t)}$ to deal with energy demands impossible to deliver.

$$E_{EV(EV,t)} + E_{EV_{rx}(EV,t)} \geq E_{EV_{min}(EV,t)} \tag{4.21}$$

The charging and discharging power rates are subject to an upper bound, as demonstrated in

$$P_{EV_{ch}(EV,t)} < P_{EV_{ch}max(EV,t)} X_{EV_{ch}(EV,t)} \tag{4.22}$$

and

$$P_{EV_{dis}(EV,t)} < P_{EV_{dis}max(EV,t)} X_{EV_{dis}(EV,t)} \tag{4.23}$$

where $X_{EV_{ch}(EV,t)}$ and $X_{EV_{dis}(EV,t)}$ represent binary variables to show if the EV is either charging or discharging, while Equation 4.24 prevents the EVs from charging and discharging simultaneously.

$$X_{EV_{ch}(EV,t)} + X_{EV_{dis}(EV,t)} \leq 1 \tag{4.24}$$

Equation 4.25 is used to keep track of the current SOC of the EV batteries, where $\eta_{EV_{ch}}$ and $\eta_{EV_{dis}}$ represent charging and discharging efficiencies, respectively.

$$\begin{aligned} E_{EV(EV,t)} =& E_{EV(EV,t-1)} + \eta_{EV_{ch}} * P_{EV_{ch}(EV,t)} \Delta t - \\ & (1/\eta_{EV_{dis}}) * P_{EV_{dis}(EV,t)} \Delta t \end{aligned} \tag{4.25}$$

To prevent overcharging and over discharging, Equations 4.26 and 4.27 are considered.

$$\eta_{EV_{ch}} P_{EV_{ch}(EV,t)} \Delta t < E_{EV_{max}(EV,t)} - E_{EV(EV,t)} \tag{4.26}$$

$$(1/\eta_{EV_{dis}}) P_{EV_{dis}(EV,t)} \Delta t < E_{EV(EV,t-1)} \tag{4.27}$$

It is important to note that Equations 4.23, 4.24, 4.27 are only used when V2G capabilities are considered. When only V1G is considered, these constraints will not be part of the optimisation.

When EVAs are also considered as entities with responsibilities on the grid, certain constraints will have to be established ensure grid efficiency and effectiveness. First, from the DSO perspective, it is necessary to include a constraint to limit the amount of contracted power $P_{EVA_{ChCont}(EVA,t)}$ that can be curtailed by the DSO, hence

$$P_{EVA_{ChCont}(EVA,t)} \leq P_{EVA_{ChCont}max(EVA,t)} \tag{4.28}$$

knowing that $P_{EVA_{ChCont}max(EVA,t)}$ is calculated taking into account the power and flexibility of each EVA, shown in Equation 4.29, where $\delta_{EVA(EVA,t)}$ represents the flexibility in the power demand of each EVA.

$$P_{EVA_{ChCont}max(EVA,t)} = P_{EVA_{demand}(EVA,t)} * \delta_{EVA(EVA,t)} \tag{4.29}$$

The sum of the power supplied and the power non supplied (contracted and non-contracted), has to be equal to $P_{EVA_{ch}(EVA,t)}$, the power demanded by the EVAs. That relation is then transformed into the constraint shown in Equation 4.30, that limits the amount of $P_{EVA_{ChNonCont}(EVA,t)}$ used by the DSO.

$$P_{EVA_{ChNonCont}(EVA,t)} \leq P_{EVA_{ch}(EVA,t)} - P_{EVA_{ChCont}(EVA,t)} \tag{4.30}$$

The power of EV discharge that the DSO can use at any period is limited to EVA's capability to supply it, as seen in Equation 4.31. $P_{EVA_{dis}avail(EVA,t)}$ represents the available power the EVAs have in their domain to discharge.

$$P_{EVA_{dis}DSO(EVA,t)} \leq P_{EVA_{dis}avail(EVA,t)} \tag{4.31}$$

From the EVA perspective, it is necessary to establish that the power of charge and discharge used by the EVA, takes into account every EV that is within the domain of each EVA. For that, the variable $A_{EV(EVA,EV,t)}$ is used to demonstrate the availability of the EVs, showing the EVA that is responsible for their management in each time step.

$$P_{EVA_{ch}(EVA,t)} = \sum_{EV=1}^{N_{EV}} P_{EV_{ch}(EV,t)} A_{EV(EVA,EV,t)} \tag{4.32}$$

$$P_{EVA_{dis}(EVA,t)} = \sum_{EV=1}^{N_{EV}} P_{EV_{dis}(EV,t)} A_{EV(EVA,EV,t)} \tag{4.33}$$

The total charge and discharge power is also limited to a maximum value, however this limitation is set at a very high rate, so as to not disturb the EVA's original power demand.

$$P_{EVA_{ch}(EVA,t)} \leq P_{EVA_{ch}max(EVA,t)} \tag{4.34}$$

$$P_{EVA_{dis}(EVA,t)} \leq P_{EVA_{dis}max(EVA,t)} \tag{4.35}$$

To calculate the EV discharge power available in each EVA, Equation 4.36 is used.

$$P_{EVA_{dis}avail(EVA,t)} = min(E_{EVA_{SOC}(EVA,t)} - E_{EVA_{SOC}min(EVA,t)}; P_{EVA_{dis}max(EVA,t)}) \tag{4.36}$$

This equation finds the minimum value between the energy available in the EVs and the maximum power discharge allowed. The energy available is calculated with the current SOC of their batteries ($E_{EVA_{SOC}(EVA,t)}$) and the minimum energy required at all times ($E_{EVA_{SOC}min(EVA,t)}$).

When flexibility is used by the DSO, the EVAs need to reschedule their EV profiles. The power that each EVA can charge in any given time step is further limited, as shown in Equation 4.37.

$$\begin{aligned} P_{EVA_{ch}max(EVA,t)} \leq P_{EVA_{ch}init(EVA,t)} - P_{EVA_{ChCont}(EVA,t)} \\ - P_{EVA_{ChNonCont}(EVA,t)} - P_{EVA_{dis}DSO(EVA,t)} \end{aligned} \tag{4.37}$$

The variable $P_{EVA_{ch}init(EVA,t)}$ represents the initial value of charging power that the EVAs send to

the DSO, upon the first optimization. After the DSO has finished optimizing its power scheduling, the EVA repeats the process with updated restrictions, taking into account the values of $P_{EVA_{ChCont}(EVA,t)}$ and $P_{EVA_{ChNonCont}(EVA,t)}$ imposed, as well as the discharge power $P_{EVA_{dis}DSO(EVA,t)}$ used.

Finally, a constraint is added to balance the overall power distribution in those hours where flexibility is used, allowing the EVA to choose the optimal balance between charging and discharging to meet power demands requested by the DSO.

$$P_{EVA_{ch}(EVA,t)} - P_{EVA_{dis}(EVA,t)} \leq P_{EVA_{ch}max(EVA,t)} \tag{4.38}$$

Regarding the model of the network, obtaining the power flow and voltage magnitude in the distribution network busses and lines is necessary to guarantee reliability and safety in all the components that make up a network, from power lines to transformers and substations. In Equation 4.39, the active power balance in each bus is calculated taking into account all the elements that produce and consume active power, considering that the EVs have V2G capabilities.

$$\begin{aligned} P(i,t) = & \sum_{GEN=1}^{N_{GEN}} P^i_{GEN(GEN,t)} - P^i_{EXC(GEN,t)}) + \\ & \sum_{LOAD=1}^{N_{LOAD}} (P^i_{RED(LOAD,t)} + P^i_{CUT(LOAD,t)} + \\ & P^i_{ENS(LOAD,t)} - P^i_{LOAD(LOAD,t)}) \\ & \sum_{EV=1}^{N_{EV}} (P^i_{EV_{dis}(EV,t)} - P^i_{EV_{ch}(EV,t)}) + \\ & \sum_{ST=1}^{N_{ST}} (P^i_{ST_{dis}(ST,t)} - P^i_{ST_{ch}(ST,t)}) + \end{aligned} \tag{4.39}$$

When the EVAs are introduced to the optimisation, the charge and discharge power of the EVs disappear from equation 4.39, being replaced by the power supplied to and received from the EVAs, $P_{EVA_{ch}(EVA,t)}$ and $P_{EVA_{dch}(EVA,t)}$.

If only V1G is considered, than the equations transforms to

$$
\begin{aligned}
P(i,t) = & \sum_{GEN=1}^{N_{GEN}} P^i_{GEN(GEN,t)} - P^i_{EXC(GEN,t)}) + \\
& \sum_{LOAD=1}^{N_{LOAD}} (P^i_{RED(LOAD,t)} + P^i_{CUT(LOAD,t)} + \\
& P^i_{ENS(LOAD,t)} - P^i_{LOAD(LOAD,t)}) - \\
& \sum_{EV=1}^{N_{EV}} (P^i_{EV_{ch}(EV,t)}) + \\
& \sum_{ST=1}^{N_{ST}} (P^i_{ST_{dis}(ST,t)} - P^i_{ST_{ch}(ST,t)}) +
\end{aligned}
\tag{4.40}
$$

where $P(i,t)$ represents the active power in each bus. As for the reactive power balance in each bus, $Q(i,t)$, it is calculated as

$$
Q(i,t) = Q^i_{GEN(GEN,t)} - Q^i_{LOAD(LOAD,t)} \tag{4.41}
$$

as only the generators produce reactive power, and only the loads consume it.

Using Kirchhoff's current law, the active power injected in each bus can be calculated as

$$
P(i,t) = V_i * \sum_{j \in L^i} V_j (G_{ij} \cos\theta_{ij} + B_{ij} \cos\theta_{ij}) \tag{4.42}
$$

where G_{ij} and B_{ij} correspond to the real and imaginary part of the admittance matrix of the network, respectively, and L^i represents the set of lines that connect to bus i. The same can be done to calculate the reactive power injected in each bus:

$$
Q(i,t) = V_i * \sum_{j \in L^i} V_j (G_{ij} \cos\theta_{ij} - B_{ij} \cos\theta_{ij}) \tag{4.43}
$$

It is also crucial to keep the voltage levels within an upper and lower limits, as well as the voltage angle, described in Equations 4.44 and 4.45.

$$
V^i_{min} \leq V_i \leq V^i_{max} \tag{4.44}
$$

$$
\theta^i_{min} \leq \theta_i \leq \theta^i_{max} \tag{4.45}
$$

To ensure that the lines don´t overheat, it is crucial to guarantee that they don't exceed their thermal limits, denoted as S^{ij}_{max}, as it is shown in Equations 4.46 and 4.47.

$$V_{i(t)}(y_{ij}V_{ij(t)} + y_{sh(i)}V_{i(t)}) \leq S^{ij}_{max} \tag{4.46}$$

$$V_{j(t)}(y_{ji}V_{ji(t)} + y_{sh(j)}V_{j(t)}) \leq S^{ji}_{max} \tag{4.47}$$

$V_{ij(t)}$ represents the voltage difference between bus i and bus j, y_{ij} and y_{ji} are the ij and ji elements of the admittance matrix, while $y_{sh(i)}$ and $y_{sh(j)}$ symbolize the shunt admittance of line in bus i and j, respectively, using the π equivalent circuit.

These constraints are then used in conjunction with the objective functions described previously, to reach the optimal solution for the models proposed.

Model	Used by	Constraints
Model 1 - V2G	DSO	4.4-4.27,4.39, 4.41-4.47
Model 1 - V1G	DSO	4.4-4.20,4.22,4.25,4.26,4.40-4.47
Model 2	DSO	4.4-4.19,4.28-4.31,4.39, 4.41-4.47
	EVA	4.20-4.27, 4.32-4.38

Table 4.2: Constraints used for each model.

4.2.3 Optimization

To address the complex challenges inherent in the management of the distribution grid and decentralized energy resources, a robust optimization approach is essential. In this study, the Mixed-Integer Non-Linear Programming (MINLP) is employed to formulate and solve the optimization problem.

It combines the modeling features of Mixed-Integer Linear Programming (MILP) and Non-Linear Programming (NLP) into a flexible modeling framework. By integrating integer variables, it becomes feasible to include discrete decisions, enabling the selection among specific options within the optimization model [55]. Moreover, by incorporating both linear and nonlinear functions, MINLP can represent a variety of objectives, making it well-suited for the diverse and dynamic nature of energy management in modern grids. By leveraging MINLP, we can simultaneously optimize the allocation of resources, such as DG units, energy storage systems, and DR programs, while considering constraints related to grid capacity, operational limits, and cost objectives.

As the scale of the optimization problem increases, particularly with the inclusion of a large number of EVs and diverse DERs, the computational complexity grows exponentially. MINLP solvers may struggle to efficiently explore the vast solution space [56], leading to prolonged optimization times. In practice, this translates to extended processing times and computational resources required to reach an optimal solution, rendering MINLP optimization impractical for real-time or day-ahead scheduling applications. The volume of decision variables and constraints involved in modeling numerous EVs, storage systems,

renewable energy sources, and demand response programs increases the computational burden, impeding the scalability of MINLP-based approaches.

The simulations were performed using MATLAB, while the optimization process was conducted using GAMS. By leveraging the capabilities of both MATLAB and GAMS, to develop and validate the deterministic optimization models and simulate various scenarios, it enables a comprehensive exploration and evaluation of the solutions proposed to address the challenges posed by the integration of electric vehicles into the grid. The proposed methodologies have been executed on a computer with a processor Intel(R) Core(TM) i7-8550U, 8GB of random-access-memory and a Windows 11 Home 64 bits operating system.

5

Case study

Contents

5.1 Distribution Network 41

5.2 Electric vehicle data 45

5.3 Electric vehicle aggregators data 46

This chapter presents the case studies that will used for testing and analysing the models previously explained, starting with the description of the distribution network and resources used, as well as all the data considered for the EV integration.

5.1 Distribution Network

The distribution grid under study comprises 37 buses, serving a total of 1908 consumers. The network is interconnected, with consumers connected to bus 1 (substation), which is the main entry point into the grid. This network was proposed by [57] and adapted by [51] to include renewable energy sources in order to analyze its integration with EVs.

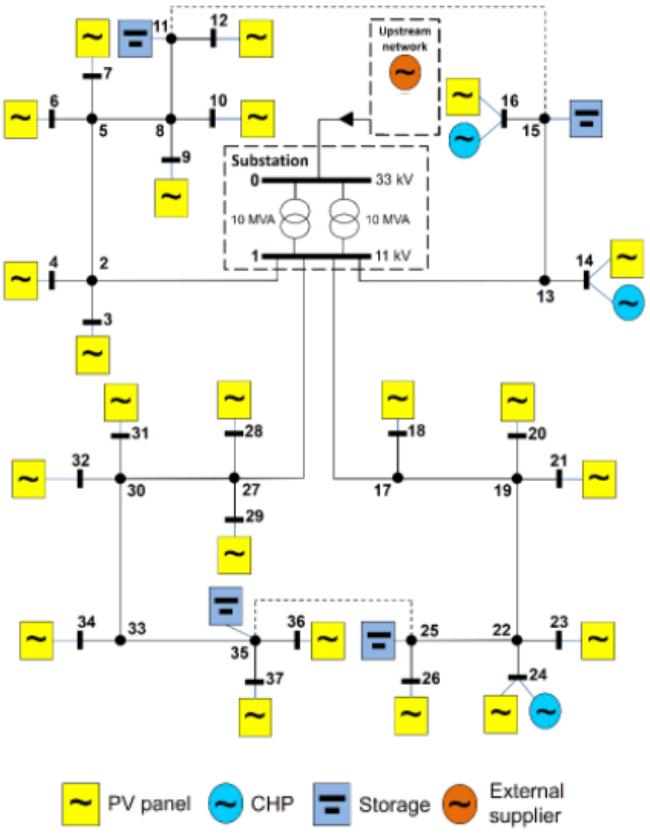

Figure 5.1: Distribution network used.

Bus 1 is equipped with two transformers, each with a capacity of 10 MVA, ensuring efficient power distribution throughout the network. Therefore, the DSO can only acquire a maximum of 20 MVA in each period, which corresponds to the total transformers capacity. The grid's infrastructure includes lines, with resistance and inductive reactance characteristics established at 0.00265 p.u./km and 0.000935 p.u./km, respectively. These parameters are multiplied by the length of each line to determine the resistance and

reactance values for individual lines. The length of each branch is shown in Annex A. The thermal limit of each line is set at 10 MVA to prevent overload. This value was set considerably high, so that the line constraint don't interfere with the EV results.

By analyzing the energy roadmap for 2050 shown in [58], the author of [51] proposed the scenario for the DG units shown in Table 5.1.

Resource	Number of Units
External Suppliers	10
PV Panels	1080
CHP	3
Storage	4

Table 5.1: Number of Resources.

In Table 5.2, the maximum power output of each type of generation is listed, as well as the cost associated with them.

Type of generator	Max Power Generated (kW)	Cost (m.u./kWh)
External Suppliers	20000	0.02-0.15
PV Panels	8090	0.08
CHP	1500	0.01-0.03

Table 5.2: Characteristics of the generator types.

There are ten external suppliers considered, each one with a maximum power generation of 2000kW, adding up to a total of 20MW. Their cost of generation starts on 0.02 m.u./kWh, and it increases with every additional supplier that is needed, going all the way up to 0.15 m.u./kWh for the tenth supplier.

For the EV panels, a forecast [59] was used to obtain power output throughout the day, resulting in the profile shown in Figure 5.2, where between 9 PM and 6 AM the PV units are not able to generate any electricity due to being night time, and reaching peak generation between 12 AM and 3 PM.

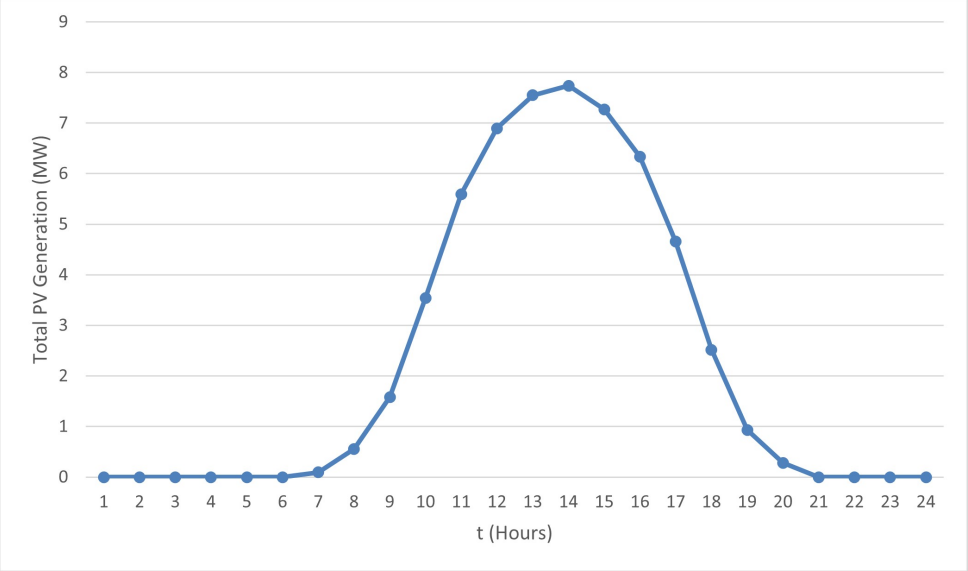

Figure 5.2: Profile of the power generated by PV panels.

The 1018 PV panels have been placed in the same buses that have the consumers, thus having 22 PV units. It has a cost of generation of 0.08 mu/kWh. On the other hand, the penalization related to the power generation curtailment of PV panels is equal to 0.10 m.u./kWh.

Three CHP units with a maximum power of 500kW are also considered, each one with a quadratic cost curve associated with them, shown in Table 5.3. This cost curve is associated with the quadratic relationships between fuel consumption and boiler loads in CHP generators [60]. They have a fixed cost that goes from 0.005 m.u./h to 0.01 m.u./h and quadratic cost from 0.005 m.u./kWh^2 to 0.01 m.u./kWh^2. A minimum power generation of 75 kW is also imposed for each CHP unit.

ID	Bus	c_A(m.u./h)	c_B(m.u./kWh)	c_C(m.u./kWh^2)
1	14	0.01	0.03	0.006
2	16	0.0015	0.02	0.01
3	24	0.005	0.01	0.005

Table 5.3: Quadratic cost of CHP generators.

There is also a cost associated with the non use of generated power, and it is 0.0001 m.u./kW, to prevent the DSO from generating excessive power.

In terms of storage, four storage systems are strategically placed at the end of each main feeder, with a maximum capacity of 250 kWh and initial energy stored level set at 200 kWh. Their minimum SOC is set at 20% of their total capacity, with the minimum SOC at the final period being 50%.

ID	Bus	Capacity(kWh)	Initial SOC (kWh)	Charge rate (kW)	Discharge rate (kW)
1	11	250	200	150	200
2	15	250	200	150	200
3	25	250	200	150	200
4	35	250	200	150	200

Table 5.4: Characteristics of the storage units.

These systems facilitate energy storage and retrieval, with charging and discharging rates capped at 150 kW and 200 kW, respectively. Charging and discharging efficiencies are established at 90%. Storage charge cost is equal to 0 m.u./kW, while its discharge cost goes from 0.55 m.u./kW to 0.65 m.u./kW.

The load profiles encompass 22 consumers with diverse consumption patterns, categorized into five distinct profiles based on usage behavior. These profiles range from domestic consumption to commercial and service-based consumption, each exhibiting unique load characteristics. This does not mean that every load in the same category has the exact same load profile, but rather that they have a similar disposition in terms of the percentage of the max load they demand on each period. In Annex A, the individual power demands of each load are shown.

The total power demand of the loads corresponds to 370,6 MWh, reaching its highest point in period 20, with a demand approximately of 22,6MW, and its lowest point in period 6, with a demand of around 8,6MW.

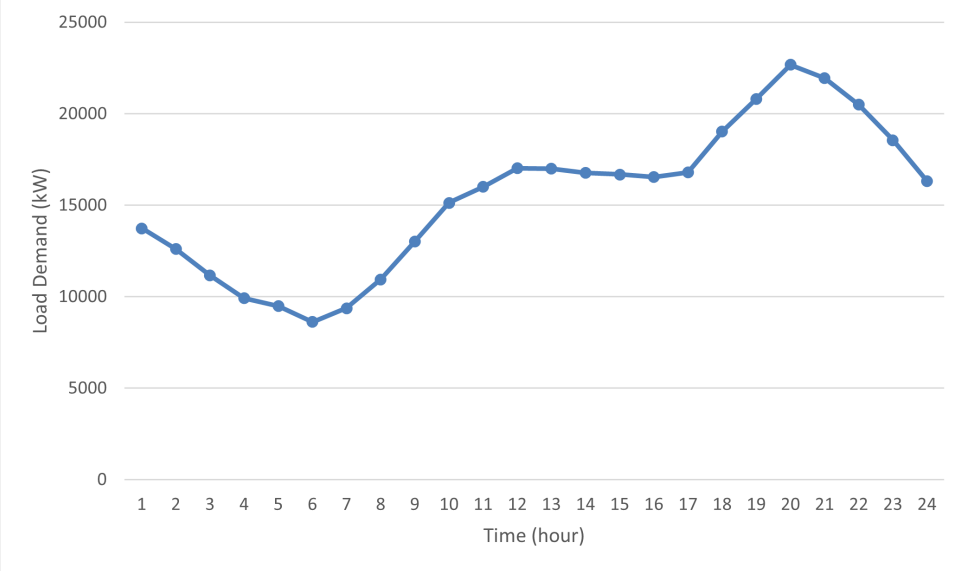

Figure 5.3: Power demand profile.

With this load profile, the total transformers capacity of 20 MVA was exceeded in certain periods, imposing the DSO to schedule decentralized resources such as DG units, EV discharging, storage, and

DR programs.

There are two different DG services considered for the loads, reduce loads and cut loads, providing flexibility in managing consumption during peak periods. These programs have a limited amount of power that can be used, being 3% for the reduce program and 2% for the cut program, but offer an alternative to the DSO, instead of simply not supplying the energy at a higher cost. The cost associated with them is 0.15 m.u./kW and 0.20 m.u./kW, respectively.

Demand Response	Max Power(% of load)	Price (m.u./kW)
Power Reduce	3%	0.15
Power Cut	2%	0.20
Power Non-Supplied	100%	1

Table 5.5: Types of demand response programs.

5.2 Electric vehicle data

The EV data utilized in this study stems from the Electric Vehicle Scenario Simulator (EVeSSi), introduced in [61]. This algorithm generates comprehensive EV profiles, capturing crucial parameters such as charge and discharge rates, energy capacity, and travel patterns.

For this, a fleet of 500 EVs, collectively possessing an energy capacity of 7.7 MWh, is considered in the dataset. This collective capacity reflects the overall storage capability of the EV fleet, crucial for evaluating the grid's ability to manage EV charging and discharging activities effectively.

The EV's capacity, charge and discharge rates considered by the EVeSSi algorithm are taken from the technical characteristics of real commercial EVs ([62–66]), where the charge and discharge rates can go from 2.2 kW to 6.6, depending on the EV.

Number of EVs	Capacity (kWh)	Charge/Discharge Rate (kW)
500	7700	2.2 - 6.6

Table 5.6: Technical characteristics of the EVs considered.

The mean remuneration for their discharge process is equal to 0.05 m.u./kWh, ensuring a fair compensation to the users that participate in the V2G program, while charging of the EVs is set at 0 m.u./kWh, as it represents a mandatory service for the DSO. It is important to note that EV discharge was set at a lower cost than the storage discharge in order to better analyze its impacts in the power scheduling, as the focus of this scenario was the EV contribution in demand response during peak hours. The relaxation cost was set at a high value of 1 m.u./kW, as ideally it is not to be considered, if the EV power demand data is correctly estimated.

A degradation cost for the batteries is also considered at 0.02 m.u./kWh. Charging and discharging

efficiencies are both standardized at 88%, ensuring efficient energy transfer between the EVs and the grid. A minimum charge level of 20% is enforced for the EVs, maintaining an 80% depth of discharge to align with manufacturer battery performance models as to not reduce the lifespan [42].

The EVs that are not traveling in a certain period are assumed as connected to the distribution network. The driving pattern considered is shown in Figure 5.4.

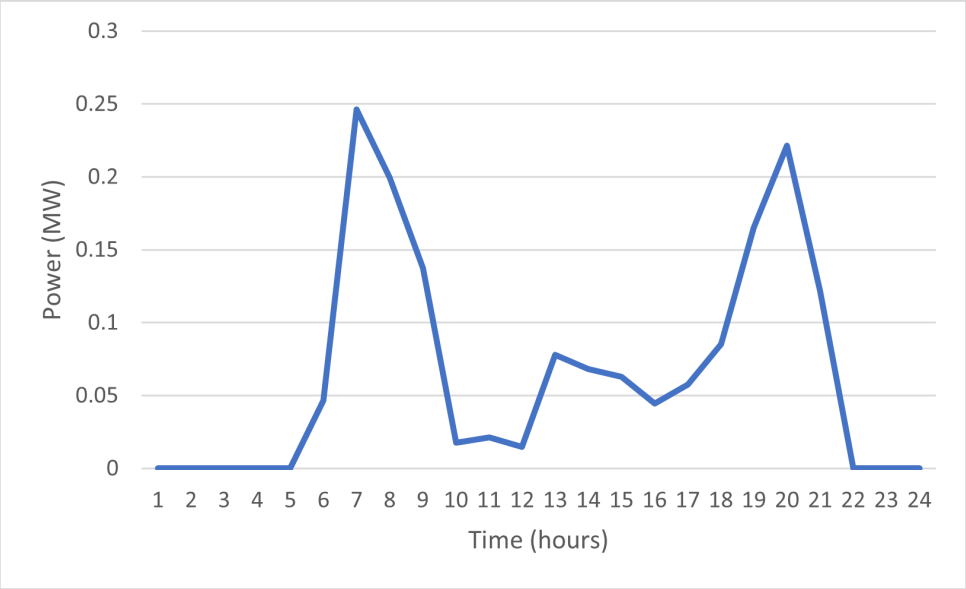

Figure 5.4: EV trip power consumption.

The total energy consumption related to the driving pattern is 1.588MWh. Seeing that the average energy consumption per kilometer travelled in the EVs considered is about 0,125kWh/km, the EVs travel, in total, about 12 704 km per day, meaning each vehicle drives approximately 25 km per day. The majority of the travelling is done between 6 AM and 10 AM, and also 6 PM and 21 PM, corresponding to the time periods that most people commute [67].

5.3 Electric vehicle aggregators data

For the distribution network shown in Figure 5.1, four EVAs are considered, each one responsible for managing the EVs in each one of the feeders. Figure 5.5 illustrates the distribution of EVAs across the network's feeders, highlighting their spatial distribution and coverage.

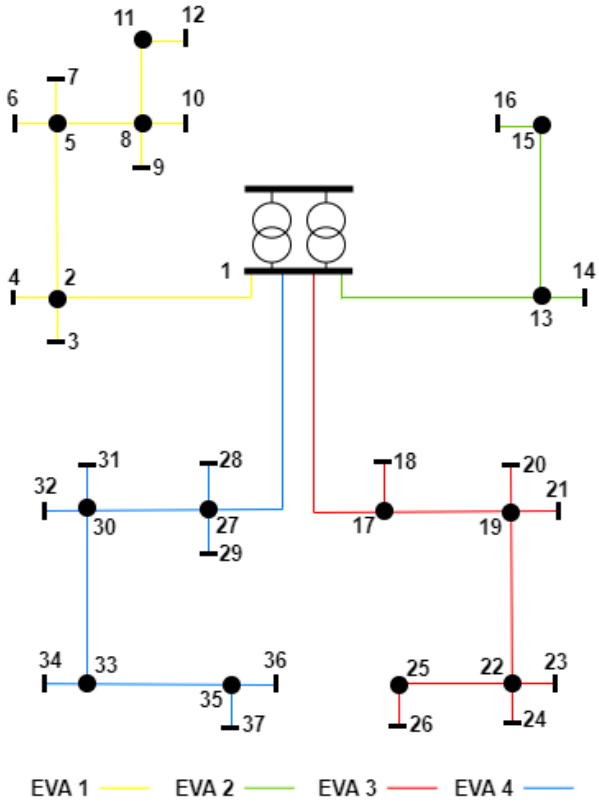

Figure 5.5: Distribution of the busses per EVA.

Figure 5.6 depicts the percentage of EVs belonging to each EVA at any given time period providing a snapshot of the distribution and allocation of EV resources across the different aggregators. The grey section of the graph represents the EVs that are not plugged in, meaning they are currently travelling and are not considered for the charging and discharging optimization by the EVA. Between periods 8 and 18, EVA 1 and EVA 3 have the biggest share of EVs under their control, meaning they are responsible for areas where the majority of people work in this specific distribution network. EVA 2 has the smallest share of EVs throughout the day, while EVA 4 represents a more residential area, having the biggest share of EVs in the periods where most people are at home.

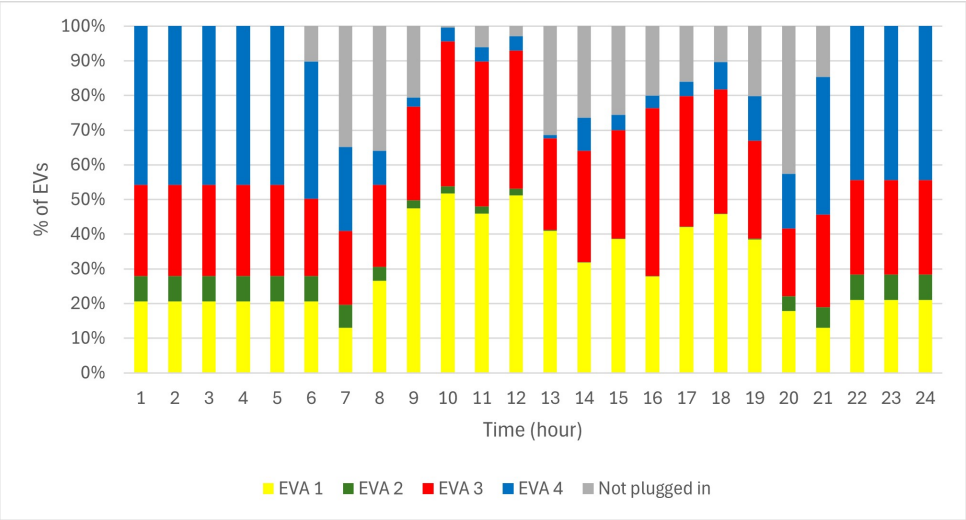

Figure 5.6: Distribution of EVs by EVAs (500 EVs).

By examining where and when EVs are active within the network, we gain insights into the demand patterns and energy consumption behaviors of the EV fleet. This analysis enables us to forecast the minimum energy levels necessary for each EVA to fulfill the energy demands of their respective EV users effectively, leveraging driving pattern data and spatial information, as shown in Figure 5.7

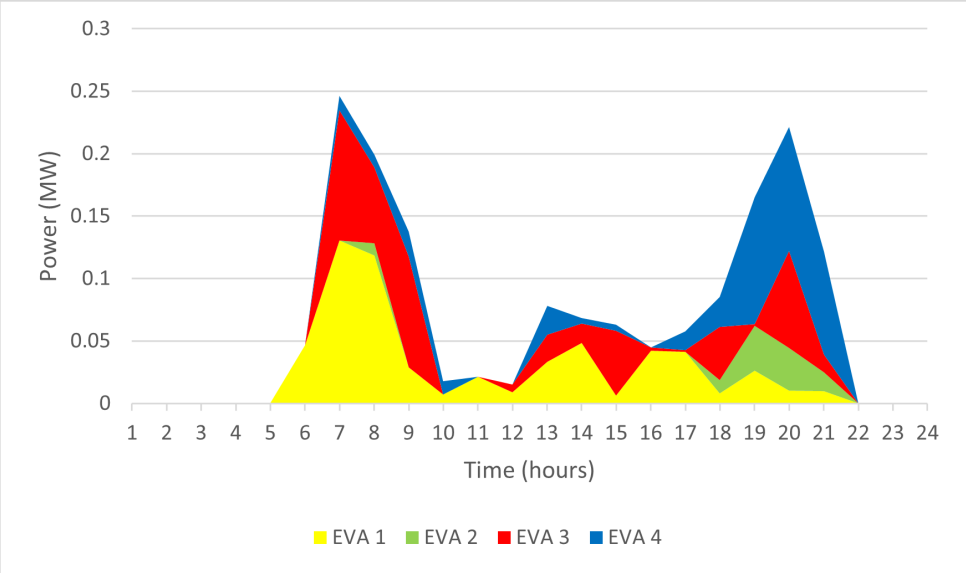

Figure 5.7: EVs driving pattern of each EVA.

EVA 1 and EVA 3 have bigger energy demand in the morning between periods 6 and 10, the periods corresponding to the time most people arrive at work. Even though EVA 2 has the smallest share of EVs, it has a considerable energy demand between periods 18 and 21. As it represents a more remote area of the network, it has less EVs under their control, but those EVs have travelled a bigger distance,

needing more energy when charging. EVA 4 has its peak energy demand around period 20.

The EVAs work as entities that have contractual agreements with the DSO, wherein the DSO supplies energy to the EVAs based on predefined terms. These terms are specified in Table 5.7.

EV Aggregator	Max Hours	Op Cost	Penalty Cost	Flexibility
EVA 1	10	0.17-0.30 m.u.	1 m.u.	5%
EVA 2	10	0.17-0.30 m.u.	1 m.u.	5%
EVA 3	10	0.17-0.30 m.u.	1 m.u.	5%
EVA 4	10	0.17-0.30 m.u.	1 m.u.	5%

Table 5.7: DSO-EVA contract information.

The opportunity cost escalates for each hour the contract is activated, culminating at 10 hours, the guaranteed hours outlined in all EVA contracts. The curve, depicted in Figure 5.8, provide insights into the dynamic nature of opportunity cost accumulation over time.

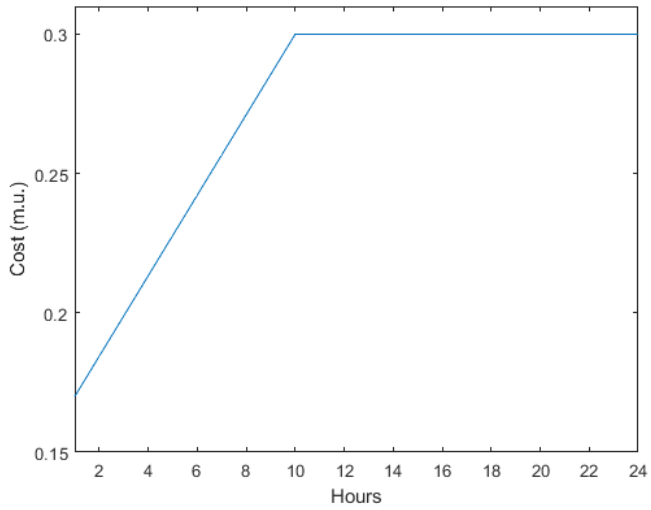

Figure 5.8: Opportunity cost curve.

Furthermore, in scenarios where the DSO cannot meet the energy demands beyond the flexibility of 5% offered by the EVAs, a penalty cost of 1 m.u./kW is incurred. This penalty mechanism incentivizes the DSO to ensure compliance with contractual obligations and mitigate the risk of energy shortfall.

As for the cost of the power that the EVAs demand from the DSO, it is used a real time electricity price curve, proportional to the consumer´s load demand, meaning the price is the lowest when demand is low (around period 6), and is the highest when the demand is high (around period 20). This curve is depicted in Figure 5.9.

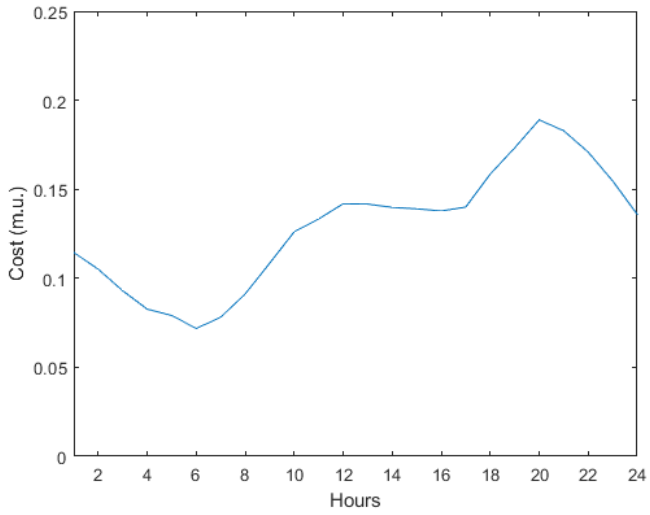

Figure 5.9: Cost of the power supplied by the DSO to the EVAs.

These data then serves as input to the optimization of the power scheduling by both the DSO and the EVAs.

6

Results

Contents

6.1 Model 1: EVs managed by DSO 53

6.2 Model 2: Coordinated DSO/EVA control of EVs 59

In this chapter, the results obtained from the simulation of the models are presented and analyzed, considering the case studies that were detailed in the last chapter. The power scheduling of each model are demonstrated, as well as the charge and discharge power of EVs and storage and the power generation used. The total cost for all entities is also analyzed, alongside the time it takes for the optimization to reach the optimal solution.

6.1 Model 1: EVs managed by DSO

The first model proposed shows us the DSO as the only entity responsible for managing power in the grid. Through detailed analysis and simulation, we explore the implications of this centralized approach on grid performance, EV integration, and the optimization of resource allocation.

6.1.1 V1G solution

When considering only V1G, the power scheduling of figure 6.1 was obtained. The brown line represents original load profile of the system, while the line in black represents the optimized power profile of the network, including the loads, DRs activated, storage charge and discharge and EV charge. Under those lines, it is shown, through different colours, the types of generation, discharge or demand responses used to fulfill that specific demand.

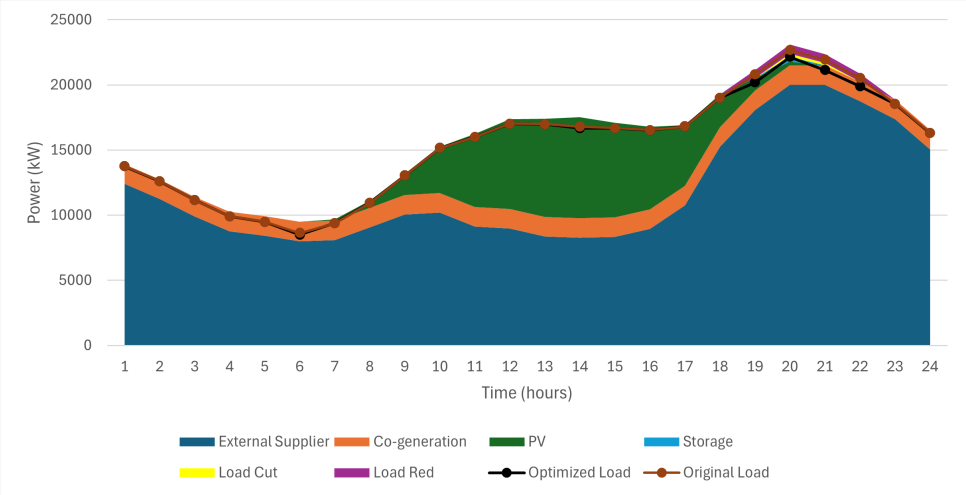

Figure 6.1: Power scheduling for Model 1 considering only V1G

By analyzing the graph, the types of generators used at the different periods of the day can be identified. Through periods 1 to 7, only external suppliers and CHP were used to supply energy. As the price of the external suppliers increases with every additional 2MW used, the DSO chooses to use them until they reach a higher price than the CHP power. When they do, the CHP power supplies the

remaining demand. Starting from period 8, the PV power becomes available. The DSO chooses to use all the PV power available, as it represents a renewable energy source with a cheaper price than the additional external suppliers. From period 10 to period 17, 36% of the power supplied came from the PVs, 9% from CHP and 55% from the external suppliers.

From period 18 onwards, the PV generation starts to fade away, as the night time starts to come. Coincidentally, the demand profile also starts to increase reaching its peak at period 20, with a power demand of around 23.4 MW. The DSO can only obtain 20 MW from the external suppliers, due to the substation's transformer limit, and 1.5 MW from the CHP units, not reaching the value of power demanded. So, it chooses two methods to reach an optimal power scheduling under these circumstances. The DSO uses the storage discharge, as well as the activation the DR programs.

Both DR program were activated, reducing the power demand in about 2.58 MWh between periods 19 and 22 with continuous regulation, and curtailing the loads in about 420kWh in periods 20 and 21 with discrete regulation. As the continuous regulation represents a cheaper option, the DSO reduced more power through it than with the discrete regulation.

As for the storage, their discharge supplies around 400 kWh to the grid, representing half their initial SOC, due to the constraint to limit the final SOC of their batteries. The storage units started the day with around 0.8 MWh of energy in their batteries, so the DSO chooses to charge them on periods with low demand as period 6, and on periods with a surplus of renewable energies, like periods 13 and 15, as shown in figure 6.2.

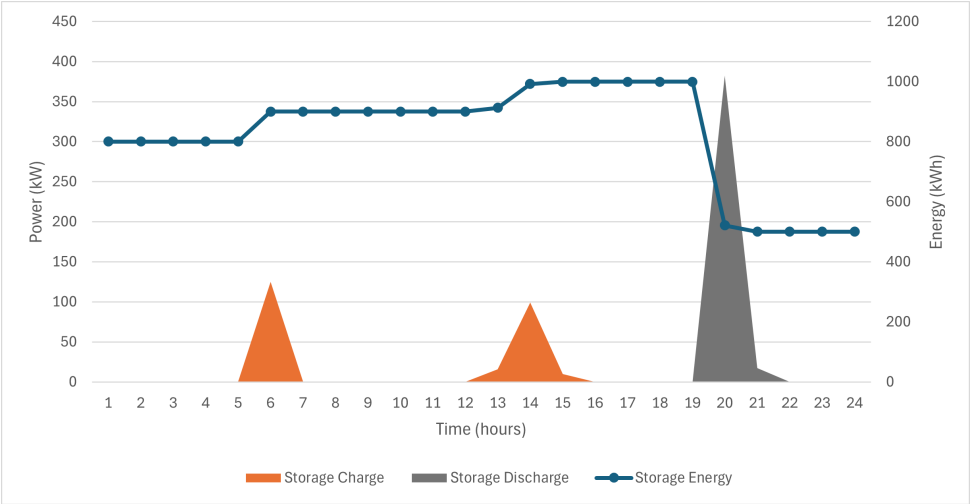

Figure 6.2: Storage scheduling for Model 1 considering only V1G

Analyzing the EV charge, shown in Figure 6.3, it is clear to see that the DSO avoided charging the EVs during peak hours where the load demand was higher. Instead opted to charge the EVs at periods with lower demand and excess PV power, between period 3 and 8, as well as between 11 and 16. The

total energy stored in all 500 EVs are also depicted in Figure 6.3 on the right axis, with the maximum value of energy being at period 6, right before a big share of the EVs starts travelling, at a value of 4.5 MWh. Its minimum level is at period 24, with 2.6 MWh stored. The minimum level is reached at the end of the day because during peak hours (19-22), the EVs were not charged to avoid power losses and grid congestion. According to the EV driving pattern shown in Figure 5.4, from period 22 onwards the EVs don't travel, meaning the DSO does not need to the charge until the next day. The total EV charging power used is around 3.5 MWh.

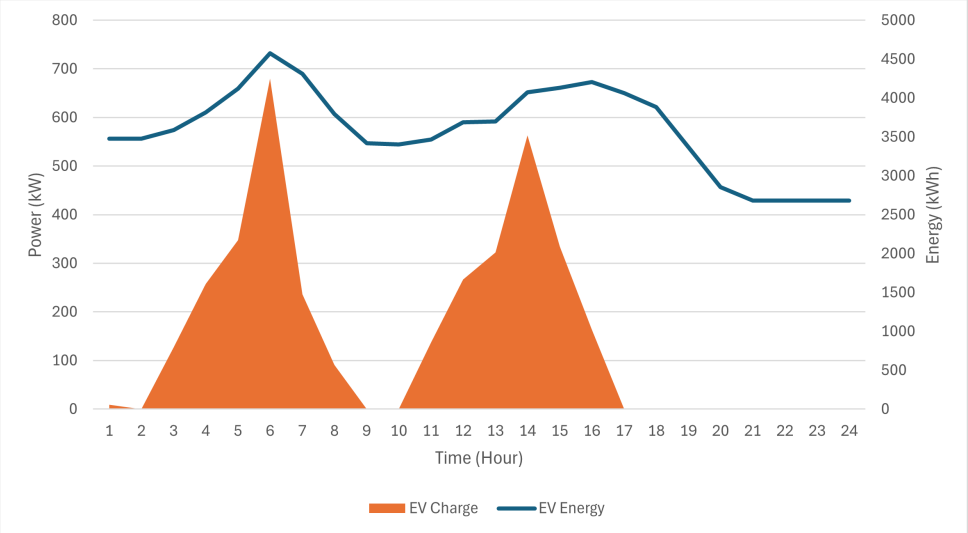

Figure 6.3: EVs scheduling for Model 1 considering only V1G

In terms of cost, the MINLP optimization reached an optimal solution of 23 396 m.u. as the total cost for the DSO. The optimization took 109 seconds to reach a solution, meaning it would take the DSO almost 2 minutes to schedule the resources for the next day in this distribution network.

6.1.2 V2G solution

Considering the use of V2G capabilities in the EVs, the power scheduling shown in Figure 6.4 was obtained.

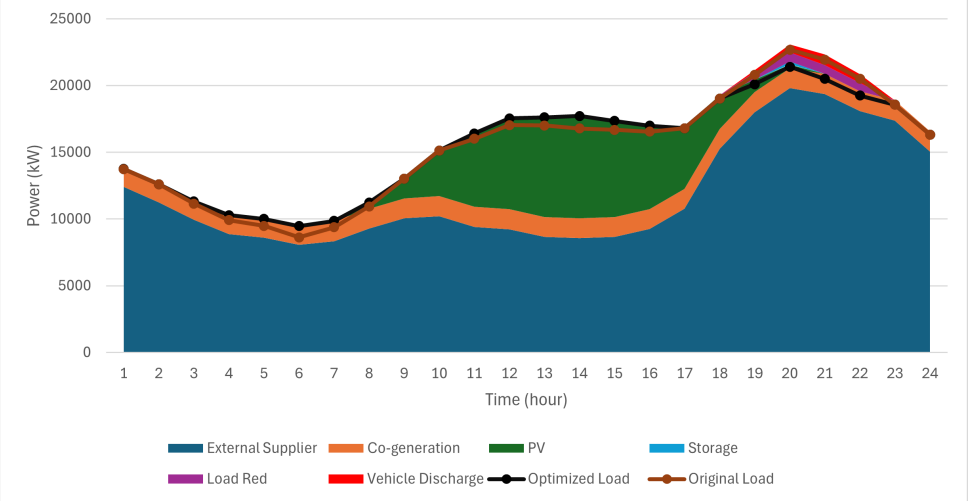

Figure 6.4: Power scheduling for Model 1 considering V2G

Allowing the EVs to supply energy back into the grid, gives the DSO a new tool to use during times of peak demand. Such use of the EVs discharge is seen in this model's power distribution. The DSO opted for using power stored in EVs between periods 19 and 22 to supply the power demanded in those hours, as the power from the generators available did not meet the total demand. EVs discharge was used in conjunction with storage discharge and demand response programs to meet the system total power demand.

The DR program used was the continuous regulation program, reducing the power demand in about 2.50 MWh between periods 19 and 22. As the DSO has access to a cheaper alternative with EV discharging, it does not use the discrete regulation to curtail the loads, unlike the previous model.

As for the storage units, their discharge supplied 240 kWh to the grid, during periods 20 and 21, as shown in Figure 6.5.

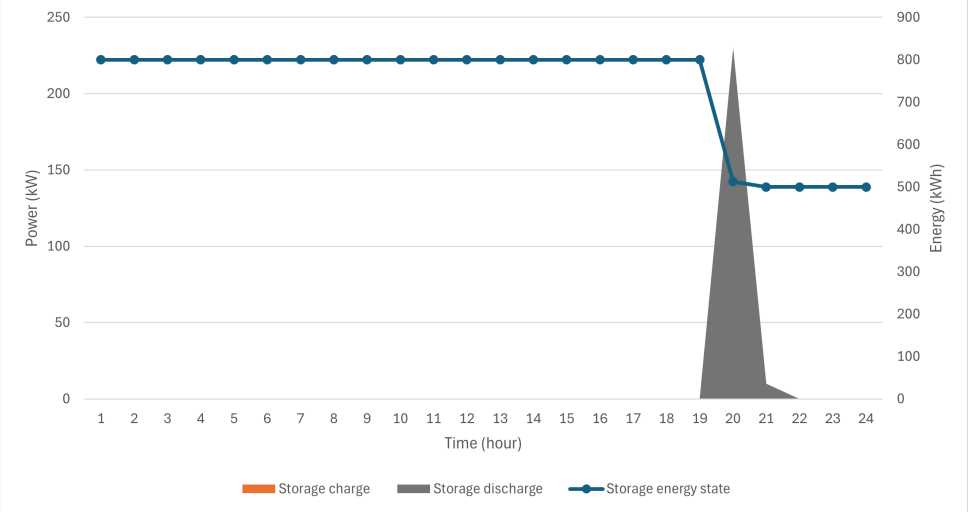

Figure 6.5: Storage scheduling for Model 1 considering V2G

The DSO did not charge the storage units at any time period during the power scheduling with V2G capabilities, as it did not need that extra power. Instead, that additional power came from the EVs batteries, as it represents a cheaper alternative.

The EVs charge pattern retain the same time periods as previously, charging between periods 3 and 8, as well as 11 and 16, but as it has to also accommodate the discharge into the grid, a higher power was used to charge their batteries. A total of 6.25 MWh were used to charge the 500 EVs, making the maximum total energy stored in their batteries of 6.6 MWh, at period 16. As the peak hours approach, the V2G starts to be implemented, discharging a total of 2.2 MWh into the grid. With this additional power, the DSO looses the need to use the maximum external supplier power available. This makes the total energy stored in the EVs drop to 2.6 MWh at the end of the day, a similar value to the one obtained without V2G, showing that the minimum energy requirements of the EVs batteries are assured.

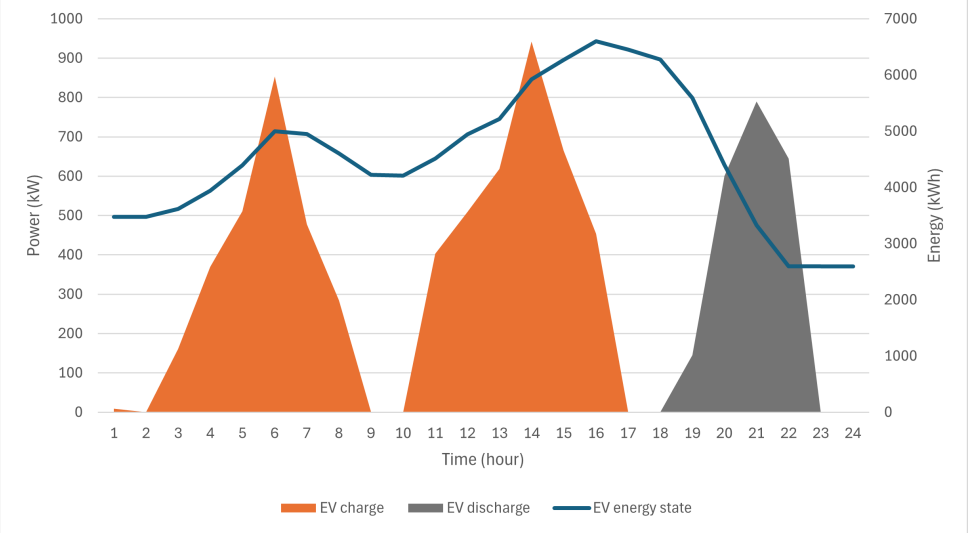

Figure 6.6: EVs scheduling for Model 1 considering V2G

In terms of cost, the MINLP optimization reached an optimal solution of 23 350 m.u. as the total cost for the DSO, a small reduction of cost compared to the V1G model due to the less DR programs activated, less use of storage energy and less need for external suppliers during peak hours. On the other hand, the MINLP optimization took 996 seconds to reach a solution, nine times longer than the V1G solution, meaning it would take the DSO a little over 16 minutes to schedule the resources with V2G capabilities for the next day in this distribution network. This increase in optimization time is due to the limitations of the MINLP algorithm in terms of efficiency to solve complex problems with a large number of resources. Even though it is still an acceptable time for the day ahead scheduling, an increase in the penetration of EVs could easily escalate the time to reach the optimal solution and make this approach not competitive for the DSO.

	Cost (m.u.)	Time (s)
Model 1 - V1G	23 396	109
Model 1 - V2G	23 350	996

Table 6.1: Comparison of cost and time of optimizations

Further details of both solutions are presented in Annex B.

To ensure that both technologies (V1G and V2G) maintain grid reliability, the voltage stability needs to be analyzed. For this, the worst case scenario was studied, meaning the period where the demand reached its peak value, corresponding to period 20. This is the period where the biggest deviation occurs between busses, as the consumption of active power is higher. Figure 6.7 shows the voltage magnitude on every bus at period 20, on both cases.

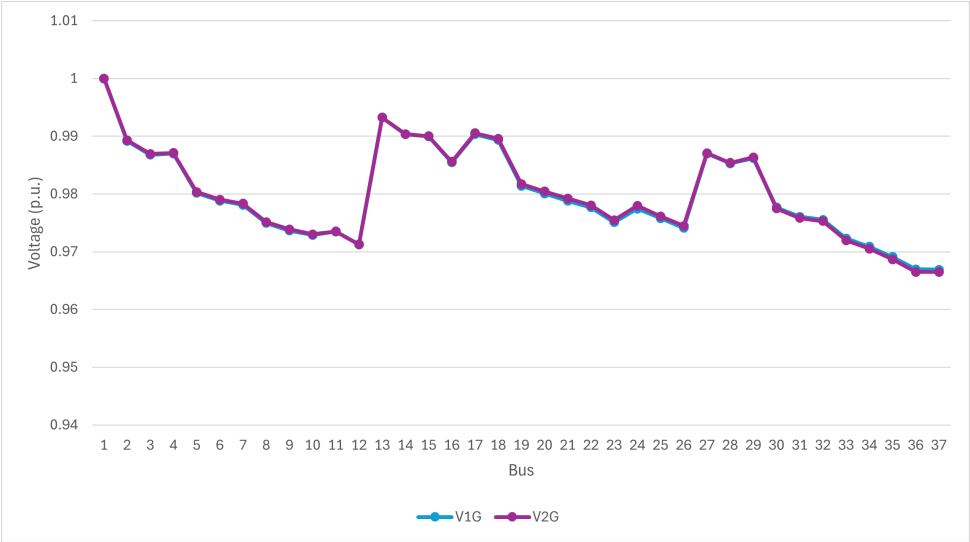

Figure 6.7: Voltage magnitude on every bus at period 20

Both technologies maintain the voltage levels in every bus within the defined limit, which is set at a deviation of 5% to avoid damage to equipment connected to the grid. The points of the distribution network further away from the main transformer correspond to the biggest deviations in voltage level, with the worst case being bus 37 with an approximate deviation of 3.3%, on both cases. Still, the reliability of the grid was not compromised.

6.2 Model 2: Coordinated DSO/EVA control of EVs

The second model proposed in this study depicts two different entities with management privileges in the grid. The DSO with management responsibilities of the generation and storage, as well as the activation of demand responsive programs, and the 4 different EVAs, located at different points of the distribution grid, with the role of controlling the charge and discharge of the EVs connected.

These two types of operators interact with each other through flexibility contracts that seek to take advantage of the EV load to mitigate grid congestion and power losses. In order to analyze the dynamic nature of these contracts, the model was simulated to obtain the scheduling for 10 days. As the opportunity cost for the DSO to use the flexibility made available by the EVAs increases the more hours it is used, at the end of each day it is updated to its new value. If no flexibility was used throughout that day, then the opportunity cost remains the same. For the first day, it is considered that no flexibility has been used yet, meaning the opportunity cost will be at the lowest value possible for all EVAs, at 0.17 m.u./kW.

The EVAs start by making their EV management considering the EV constraints explained in Chapter 4, resulting in the power scheduling depicted in Figure 6.8.

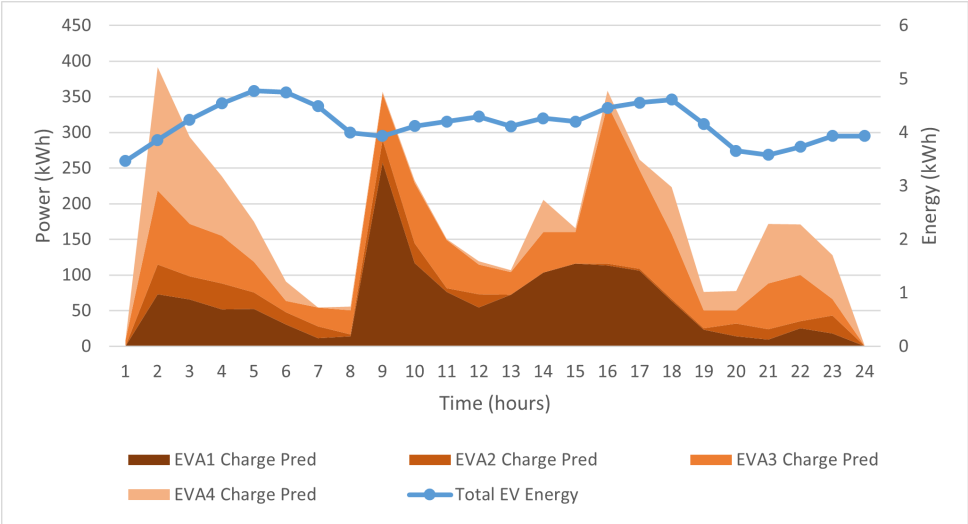

Figure 6.8: EV charge profile on the first EVA scheduling

The EVAs need to ensure that the EVs have enough energy for their next trip, without violating the minimum energy requirement. As EVs change busses throughout the day, the EVA that is responsible for their charging also changes. This leads to a total demand of 4.1 MWh for all EVAs combined. As EVAs do not account for grid limitations, their charging profile is much more spread out than in Model 1, with the peaks of charging happening in periods 2,9 and 16. The costs estimated for each EVA is shown in Table 6.2, as well as the power used for EV charging by each one of them.

	Cost (m.u.)	Charging Power (kW)
EVA 1	184	1471
EVA 2	38	329
EVA 3	184	1413
EVA 4	113	900

Table 6.2: Optimization cost and power demand predicted by the EVAs

Considering this first optimization by the EVAs, the DSO then makes its power scheduling to accommodate the EV power demand, alongside the management of the other resources, such as loads and generation. This optimization is simulated for 10 days, to see the effect of the increase in opportunity cost on resource allocation of the DSO. Figure 6.9 represents the evolution of flexibility used by the DSO.

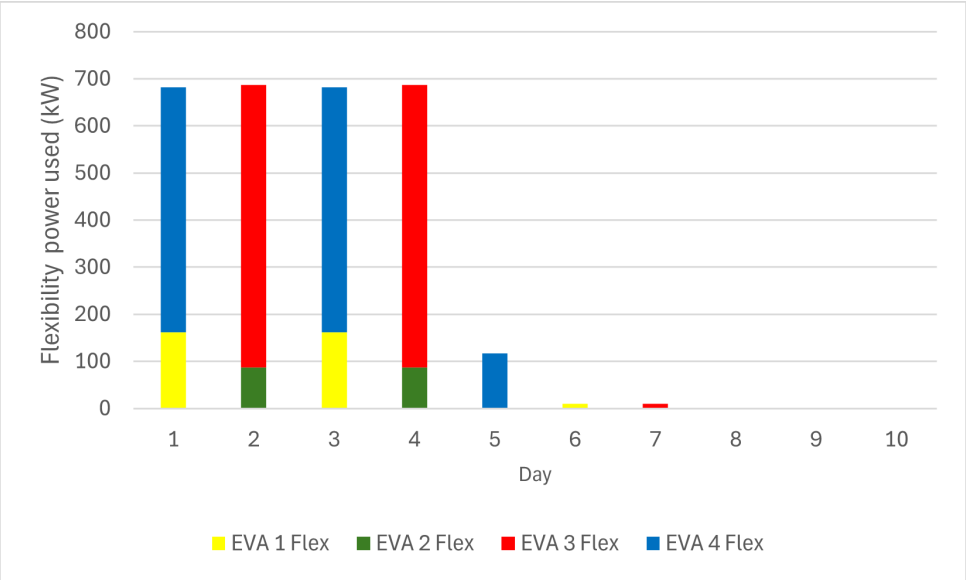

Figure 6.9: EVA flexibility used throughout the days simulated by the DSO

Taking into account the flexibility used in each day, Figure 6.10 shows the evolution of the opportunity cost throughout the days simulated.

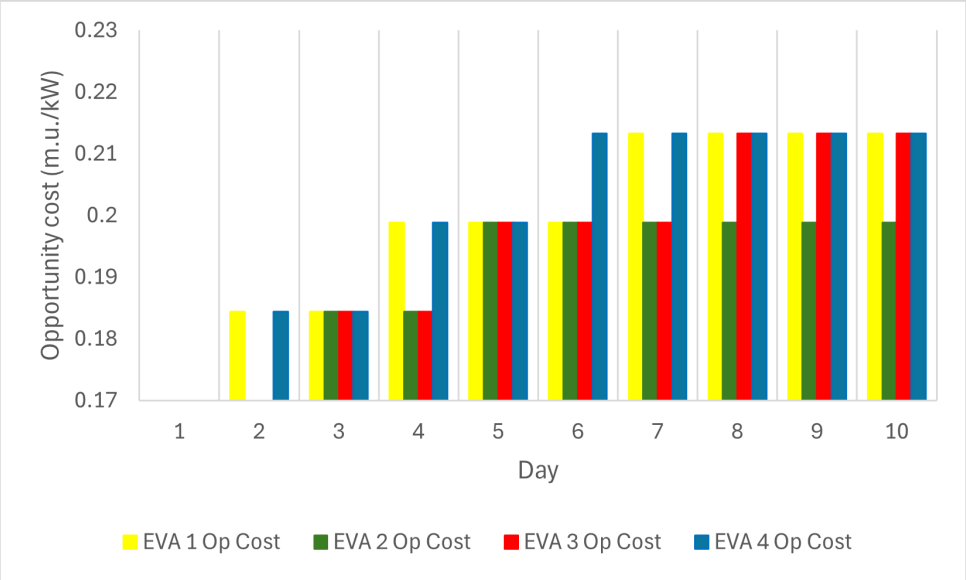

Figure 6.10: Evolution of the opportunity cost throughout the 10 days simulated

As the opportunity cost starts off low, the DSO chooses to use the flexibility on day 1, using about 690 kWh of the flexibility offered by the EVAs between periods 20 and 21, resulting in the power scheduling shown in Figure 6.11.

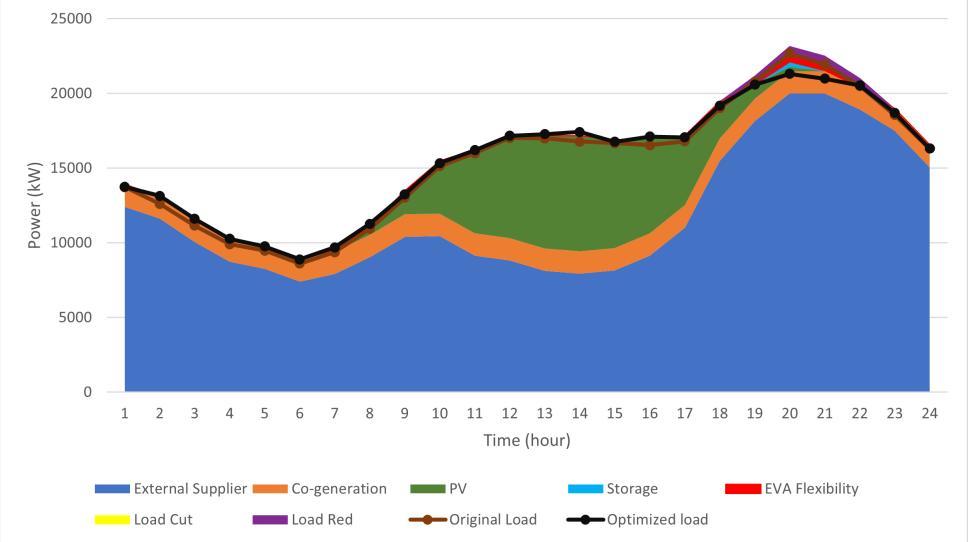

Figure 6.11: Power scheduling by the DSO for days 1-4

The opportunity cost starts off the same for all EVAs, meaning whatever flexibility it chooses to activate, it will imply the same cost. On day 1, it activates the power curtailment offered by EVA 1 and EVA 4. The rest of the demand in those peak hours is reached with storage discharge (400 kWh), as well as the activation of the DR programs (about 2.5 MWh), all in between these periods of high demand. This results in a total cost of optimization of 23 518 m.u. for the DSO. In Annex B, the detailed results for the DSO scheduling are shown.

As EVA 1 and EVA 4 had their power supply curtailed, they need to adapt to these restrictions imposed by the DSO, meaning a new optimization must take place.

EVA 1 now needs to account for the power limitation imposed in periods 20 and 21. For this, it reschedules the EV charging according to Figure 6.12, where the original charging profile is also shown to highlight its differences. To avoid the rescheduling causing perturbations in the grid by increasing the power in periods where flexibility was not used, a constraint was imposed to limit the maximum power when the demand is higher. This constraint limits the charging power of the second optimization to the original power prediction, but only on critical periods. These periods are set to be the hours where the demand passes the threshold of 20 MW (transformer capacity), and occur between periods 19 and 22.

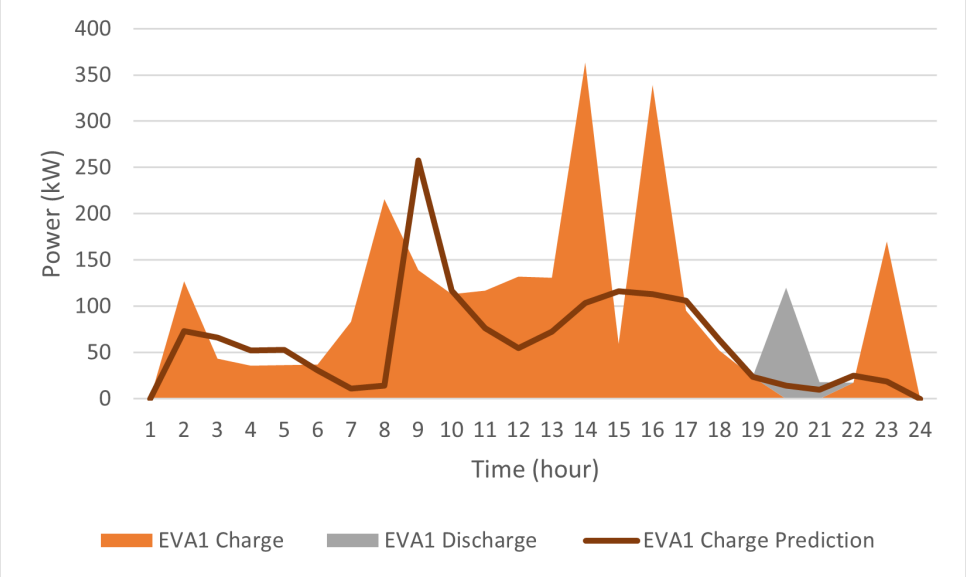

Figure 6.12: EV charging and discharging schedule by EVA 1 for day 1

To meet the power constraints imposed, EVA 1 decides to discharge the EV batteries on the periods where those constraints were added. As EVs need to meet their minimum energy requirements, additional power needs to used for their charging throughout the day, increasing the power demand in the other periods where flexibility was not used. This makes charging power used increase to 2.3 MWh, from the original 1.5 MWh. During periods 20 and 21, a total discharge of 140 kWh was made to comply with the DSO's restrictions. As the EVA needs to buy more energy supply from the DSO and also pay the EV users for the discharge of their batteries, the total cost of optimization also increases to 301 m.u. from the original 184 m.u. predicted.

Finally, EVA 4 reschedules its charging profile, considering the restrictions imposed on period 20 and 21, similarly to EVA 1. This results in the power scheduling represented in Figure 6.13. The cost of optimization increases to 385 m.u., with a total charging power of 2.4 MWh and a discharge power of 400 kWh during those periods of curtailment.

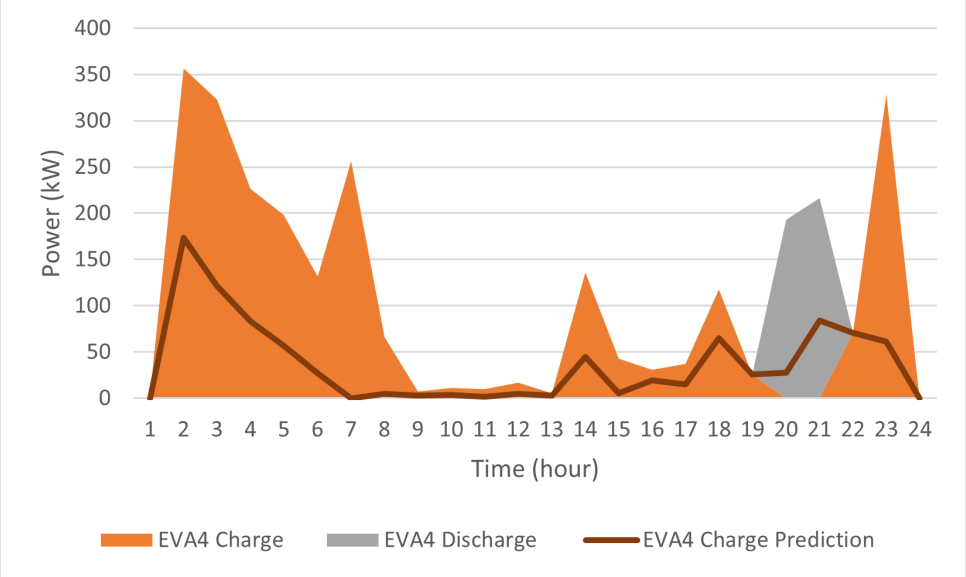

Figure 6.13: EV charging and discharging schedule by EVA 4 for day 1

EVA 2 and EVA 3 did not suffer any power curtailment, so their original scheduling does not need to be updated.

Moving on to day 2, the DSO decides to activate the same amount of flexibility as in day 1, but this time on EVA 2 and EVA 3. This is due to the fact that the opportunity cost increased on the EVAs previously used. The power scheduling is the same as in Figure 6.11, with the same amount of storage and DR programs used, on the same periods, resulting in the same total cost of 23 402 for the DSO.

EVA 1 and EVA 4 maintain their original power profile, as no restriction was imposed. On the other hand, EVA 2 and EVA 3 must reschedule the charging of EVs to meet these new restrictions. These new profiles are shown in Figures 6.14 and 6.15. The new optimizations increase the cost for EVA 2 to 63 m.u., and for EVA 3 to 359 m.u., while representing a total EV charging power of 570 kWh and 2.8 MWh, respectively. To meet the DSO restriction during periods 20 and 21, EVA 2 discharged 55 kWh from the EV batteries, while EVA 3 discharged 517 kWh.

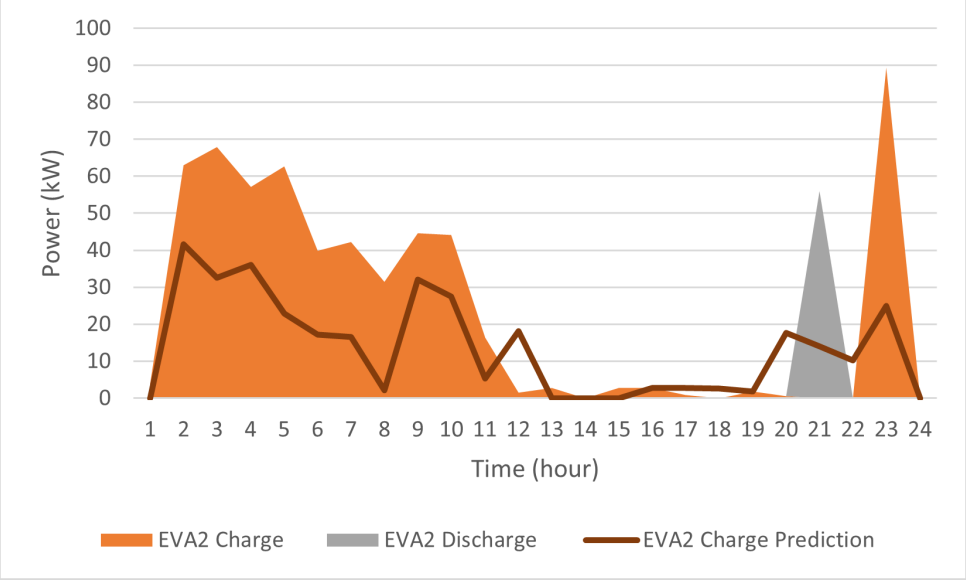

Figure 6.14: EV charging and discharging schedule by EVA 2 for day 2

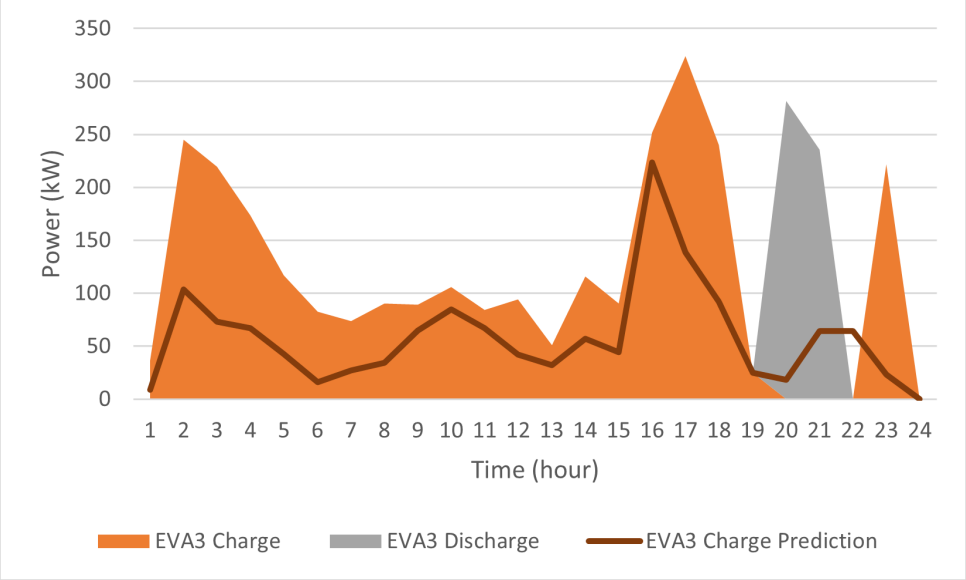

Figure 6.15: EV charging and discharging schedule by EVA 3 for day 2

At the end of day 2, the opportunity costs are the same for all EVAs, so the process repeats, with the DSO using the flexibility of EVA 1 and EVA 4 on day 3, followed by EVA 2 and EVA 3 on day 4. As this cost grows higher, so does the total cost of optimization for the DSO, reaching 23 528 m.u. during day 3 and 4.

By day 5, the opportunity cost has reached a value high enough that the DSO has better alternatives to meet the demand at those peak hours, such as the activation of DR programs with discrete regulation. This makes the use of flexibility decrease, only needing to activate it in EVA 4. The further increase in

use, makes the flexibility less and less attractive for DSO, forcing it not to rely on power curtailment on EV charging to meet high power demands in peak hours, possibly compromising the energy requirements of the EV batteries.

By day 8, no flexibility is activated, thus not requiring the EVAs to change their initial charging profile. This comes at a cost for the DSO, as now it needs more expensive options to reach the demand in those peak hours. Figure 6.16 depicts the scheduling made by the DSO for these final days, where no curtailment was made in the EV charging.

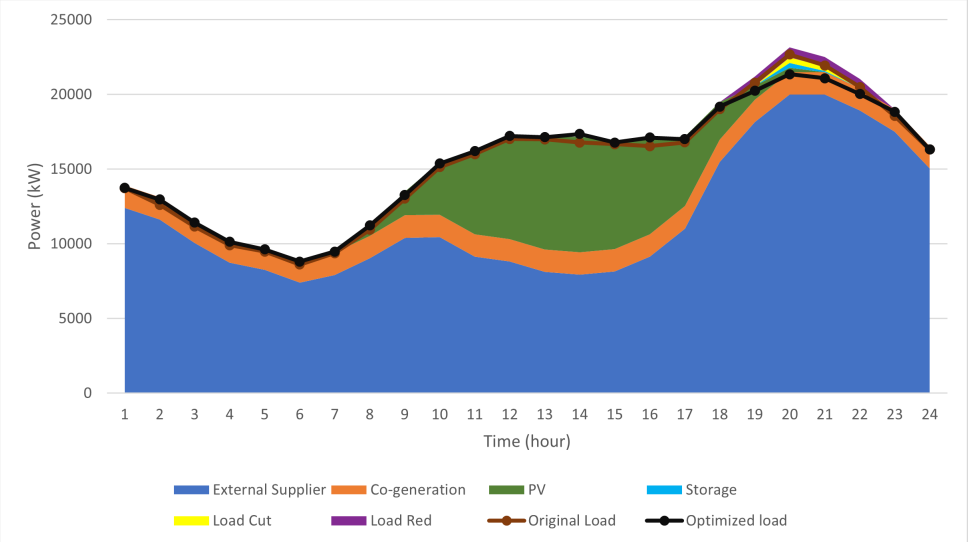

Figure 6.16: Power scheduling by the DSO for days 8-10

Table 6.3 shows the optimization cost evolution for the DSO and EVAs throughout the 10 days simulated. The underlined values represent the cost of the EVAs that had flexibility activated and made adjustments to their EV charging profile.

	1	2	3	4	5	6	7	8	9	10
DSO Cost	23518	23518	23528	23528	23535	23535	23535	23537	23537	23537
EVA 1 Cost	301	184	301	184	184	294	184	184	184	184
EVA 2 Cost	38	63	38	63	38	38	38	38	38	38
EVA 3 Cost	184	359	184	359	184	184	277	184	184	184
EVA 4 Cost	285	113	285	113	203	113	113	113	113	113

Table 6.3: Optimization cost for the DSO and EVAs throughout the days (in m.u.)

Analyzing the optimization times for the DSO for all days simulated, shown in Table 6.4, we get an average of 9.9 seconds. This corresponds to a significant reduction compared to the times presented in Table 6.1 for Model 1.

	Average Time (seconds)
DSO	9.9
EVA 1	2.8
EVA 2	3.8
EVA 3	3.0
EVA 4	3.0

Table 6.4: Average time of optimization in Model 2

This reduction is attributed to the less number of resources that need to be accounted for in the optimization, showing that the decentralized approach of Model 2 greatly decreases the burden on the operators of distribution grids when managing EVs. The optimization times for the EVAs is in average about 3.2 seconds. As EVAs only account for constraints related to EV batteries and power limitations imposed, their optimization time is still competitive, even with a large penetration of EVs.

This decentralized model greatly improves the time to reach the optimization for the day ahead scheduling, while also providing the DSO with flexibility to manage high demand periods to avoid grid stability problems, even though it can reduce some capability to fully utilize EVs to optimally reduce its costs. This happens due to the introduction of EVAs that minimize costs from their perspective. This can be seen by the increase in cost for the DSO from the first model to the second. In terms of costs for EVAs, the results show a significant increase on days where flexibility is activated, as additional power must be demanded from the DSO on other periods, as well as the remuneration of EV users for taking part in the discharge process. The opportunity cost serves as a compensation for this additional expenses imposed by the incapability of the DSO to meet the contractual power needs stipulated.

7

Conclusion

The electrification of transportation and the integration of EVs into distribution grids represent a transformative shift in the energy landscape. Through the exploration of two distinct models, this thesis aims to provide valuable insights into the complex dynamics of EV-grid integration. These models help analyze possible solutions to accommodate the rising number EVs without compromising the proper functioning of an energy grid.

In Model 1, the role of the DSO is studied as a centralized control entity. The simulation analyses both types of technologies suggested in recent studies, them being the use of smart charging and smart discharging (V1G and V2G). It revealed the promising advantages that the use of EV batteries to supply energy back into the grid can have in terms of energy allocation from renewable energies generated on low demand off peak hours into high demand peak hours, diminishing the use of other programs to curtail power from other consumers, allowing for a reduction in terms of cost of operation for the DSO when compared to the smart charging solution. But it adds a level of complexity to the optimization that can significantly affect the ability of the DSO to make the day ahead energy schedule. As a result, alternative optimization techniques, such as heuristic algorithms and metaheuristics [68] may be more suitable for handling large-scale optimization problems involving EVs. Another disadvantage is the decrease in the lifespan of the batteries for consumers, something that is compensated by the operator with an extra cost.

In Model 2, where control is decentralized to EVAs that hold contracts with the operator, the results underscored the importance of distributed optimization strategies and the potential for increased flexibility and resilience in EV-grid interactions. The aggregators add a level of flexibility through their contracted power that allow the grid to more easily adapt to sudden increases in load demand or power curtailment. It allows the DSO to make a better power dispatch for the day ahead schedule by giving it an easier way to change demand in certain parts of the grid that need to reduce consumption in order to accommodate the dynamic power fluctuations. It takes computational burden from the operator, allowing it to make the optimization problem much simpler and quicker.

Both models provided good results and served as good demonstration of how the EVs can impact the distribution grid and how they can be used in the future as a cornerstone of demand responsive services to accommodate the current expansion of networks.

Although the results were good, some other areas can be explored in future to further evaluate the role of EVs in power networks. One is to study the use of other optimization algorithms to increase the computational times and make the scheduling a simpler process for the operators. To test how the models handle uncertainty, the implementation of a stochastic problem could assess the reliability of the formulations studied. Furthermore, the application of the EVA methodology in a bigger network with a bigger penetration of EVs is also a possible next step in the study of the interaction DSO-EVA, as well as the interaction with other types renewable energies, beyond solar.

Bibliography

[1] D. J. Wuebbles and A. K. Jain, "Concerns about climate change and the role of fossil fuel use," *Fuel Processing Technology*, vol. 71, no. 1, pp. 99–119, 2001, fuel science in the year 2000: Where do we stand and where do we go from here? [Online]. Available: https://www.sciencedirect.com/science/article/pii/S0378382001001394

[2] "Power Sector Accelerating E-mobility," 2022, (Consulted: January 2023). [Online]. Available: https://www.eurelectric.org/media/5704/power_sector_accelerating_e-mobility-2022_eyeurelectric_report-2022-030-0059-01-e.pdf

[3] J. Hu, H. Morais, T. Sousa, and M. Lind, "Electric vehicle fleet management in smart grids: A review of services, optimization and control aspects," *Renewable and Sustainable Energy Reviews*, vol. 56, pp. 1207–1226, 2016. [Online]. Available: https://www.sciencedirect.com/science/article/pii/S1364032115013970

[4] "The Home of Europe's best EV policies," 2022, (Consulted: December 2022). [Online]. Available: https://monta.com/uk/blog/europe-best-ev-policies-welcome-evland/

[5] "Benefits for Electric Cars in the European Union," 2022, (Consulted: December 2022). [Online]. Available: https://www.evexpert.eu/eshop1/knowledge-center/benefits-for-electric-cars-in-the-european-union

[6] "Electric Vehicles and the Energy," 2016, (Consulted: December 2022). [Online]. Available: https://www.eea.europa.eu/publications/electric-vehicles-and-the-energy

[7] J. Cui, Y. Li, W. Zhang, and C. Chen, "Research on impact and utilization of electric vehicle integration into power grid," in *2018 Chinese Control And Decision Conference (CCDC)*, 2018, pp. 1594–1597.

[8] P. Siano, "Demand response and smart grids—a survey," *Renewable and Sustainable Energy Reviews*, vol. 30, pp. 461–478, 2014. [Online]. Available: https://www.sciencedirect.com/science/article/pii/S1364032113007211

[9] D. Stanelyte, N. Radziukyniene, and V. Radziukynas, "Overview of demand-response services: A review," *Energies*, vol. 15, no. 5, 2022. [Online]. Available: https://www.mdpi.com/1996-1073/15/5/1659

[10] "Power risk demands a real-time response," 2020, (Consulted: January 2023). [Online]. Available: https://sumitomoelectric.com/articles/technologies-for-demand-response-to-stabilize-power-supply

[11] M. H. Albadi and E. F. El-Saadany, "Demand response in electricity markets: An overview," in *2007 IEEE Power Engineering Society General Meeting*, 2007, pp. 1–5.

[12] R. Deng, Z. Yang, M.-Y. Chow, and J. Chen, "A survey on demand response in smart grids: Mathematical models and approaches," *IEEE Transactions on Industrial Informatics*, vol. 11, no. 3, pp. 570–582, 2015.

[13] T. Ericson, "Direct load control of residential water heaters," *Energy Policy*, vol. 37, no. 9, pp. 3502–3512, 2009, new Zealand Energy Strategy. [Online]. Available: https://www.sciencedirect.com/science/article/pii/S0301421509002201

[14] H. Aalami, M. P. Moghaddam, and G. Yousefi, "Demand response modeling considering interruptible/curtailable loads and capacity market programs," *Applied Energy*, vol. 87, no. 1, pp. 243–250, 2010. [Online]. Available: https://www.sciencedirect.com/science/article/pii/S030626190900244X

[15] J. Saebi, H. Taheri, and S. Nayer, "Demand bidding/buyback modeling and its impact on market clearing price," 01 2011, pp. 791 – 796.

[16] R. Tyagi and J. W. Black, "Emergency demand response for distribution system contingencies," in *IEEE PES TD 2010*, 2010, pp. 1–4.

[17] A. Dubey, S. Santoso, M. P. Cloud, and M. Waclawiak, "Determining time-of-use schedules for electric vehicle loads: A practical perspective," *IEEE Power and Energy Technology Systems Journal*, vol. 2, no. 1, pp. 12–20, 2015.

[18] K. Herter, "Residential implementation of critical-peak pricing of electricity," *Energy Policy*, vol. 35, no. 4, pp. 2121–2130, 2007. [Online]. Available: https://www.sciencedirect.com/science/article/pii/S0301421506002783

[19] H. Allcott and L. Katz, "Real time pricing and electricity markets," 01 2009.

[20] W. Zhong, R. Yu, S. Xie, Y. Zhang, and D. K. Y. Yau, "On stability and robustness of demand response in v2g mobile energy networks," *IEEE Transactions on Smart Grid*, vol. 9, no. 4, pp. 3203–3212, 2018.

[21] C. Zhou, K. Qian, M. Allan, and W. Zhou, "Modeling of the cost of ev battery wear due to v2g application in power systems," *IEEE Transactions on Energy Conversion*, vol. 26, no. 4, pp. 1041–1050, 2011.

[22] S. Sarabi, A. Bouallaga, A. Davigny, B. Robyns, V. Courtecuisse, Y. Riffonneau, and M. Régner, "The feasibility of the ancillary services for vehicle-to-grid technology," in *11th International Conference on the European Energy Market (EEM14)*, 2014, pp. 1–5.

[23] P. Wirasanti, "Ancillary services analysis based on multiple-area of v2g operation - frequency regulation service," in *IECON 2019 - 45th Annual Conference of the IEEE Industrial Electronics Society*, vol. 1, 2019, pp. 2132–2137.

[24] "Spinning reserve," 2013, (Consulted: January 2023). [Online]. Available: https://energystorage.org/spinning-reserve/

[25] W. Zhang, K. Spence, R. Shao, and L. Chang, "Optimal scheduling of spinning reserve and user cost in vehicle-to-grid (v2g) systems," in *2018 IEEE Energy Conversion Congress and Exposition (ECCE)*, 2018, pp. 1058–1064.

[26] B. Zhou, D. Yang, S. Bu, G. Du, and T. Littler, "The impact of electric vehicle uncertainties on load levelling in the uk," in *2017 IEEE Power Energy Society General Meeting*, 2017, pp. 1–5.

[27] C. S. Ioakimidis, D. Thomas, P. Rycerski, and K. N. Genikomsakis, "Peak shaving and valley filling of power consumption profile in non-residential buildings using an electric vehicle parking lot," *Energy*, vol. 148, pp. 148–158, 2018. [Online]. Available: https://www.sciencedirect.com/science/article/pii/S0360544218301567

[28] U. o. M. Center for Sustainable Systems, "U.s. grid energy storage factsheet," 2023. [Online]. Available: https://css.umich.edu/publications/factsheets/energy/us-grid-energy-storage-factsheet

[29] M. H. Athari and Z. Wang, "Modeling the uncertainties in renewable generation and smart grid loads for the study of the grid vulnerability," in *2016 IEEE Power Energy Society Innovative Smart Grid Technologies Conference (ISGT)*, 2016, pp. 1–5.

[30] K. Wali, R. Koubaa, and L. Krichen, "Cost benefit smart charging schedule for v2g applications," in *2019 16th International Multi-Conference on Systems, Signals Devices (SSD)*, 2019, pp. 34–39.

[31] S. Rahman and Y. Teklu, "Role of the electric vehicle as a distributed resource," in *2000 IEEE Power Engineering Society Winter Meeting. Conference Proceedings (Cat. No.00CH37077)*, vol. 1, 2000, pp. 528–533 vol.1.

[32] M. S. Koroma, D. Costa, G. Cardellini, and M. Messagie, “Life cycle assessment of lithium-ion battery pack: Implications of second-life and changes in charging electricity,” in *2021 IEEE Vehicle Power and Propulsion Conference (VPPC)*, 2021, pp. 1–6.

[33] K. Smith, Y. Shi, and S. Santhanagopalan, “Degradation mechanisms and lifetime prediction for lithium-ion batteries — a control perspective,” in *2015 American Control Conference (ACC)*, 2015, pp. 728–730.

[34] R. A. Verzijlbergh, M. O. W. Grond, Z. Lukszo, J. G. Slootweg, and M. D. Ilic, “Network impacts and cost savings of controlled ev charging,” *IEEE Transactions on Smart Grid*, vol. 3, no. 3, pp. 1203–1212, 2012.

[35] X. Huang, Y. Fu, J. Zhang, K. He, H. Cheng, and H. Zhang, “The impact of electric vehicle development on grid load power and electricity consumption,” in *2019 12th International Conference on Intelligent Computation Technology and Automation (ICICTA)*, 2019, pp. 158–161.

[36] M. Zou, Y. Yang, M. Liu, W. Wang, H. Jia, X. Peng, S. Su, and D. Liu, “Optimization model of electric vehicles charging and discharging strategy considering the safe operation of distribution network,” *World Electric Vehicle Journal*, vol. 13, no. 7, 2022. [Online]. Available: https://www.mdpi.com/2032-6653/13/7/117

[37] S. Sachan and N. Adnan, “Stochastic charging of electric vehicles in smart power distribution grids,” *Sustainable Cities and Society*, vol. 40, pp. 91–100, 2018. [Online]. Available: https://www.sciencedirect.com/science/article/pii/S221067071830338X

[38] Y. Yao, W. Gao, and Y. Li, “Optimization of phev charging schedule for load peak shaving,” in *2014 IEEE Conference and Expo Transportation Electrification Asia-Pacific (ITEC Asia-Pacific)*, 2014, pp. 1–6.

[39] Q. Dang, “Electric vehicle (ev) charging management and relieve impacts in grids,” in *2018 9th IEEE International Symposium on Power Electronics for Distributed Generation Systems (PEDG)*, 2018, pp. 1–5.

[40] W. Yin, Z. Ming, and T. Wen, “Scheduling strategy of electric vehicle charging considering different requirements of grid and users,” *Energy*, vol. 232, p. 121118, 2021. [Online]. Available: https://www.sciencedirect.com/science/article/pii/S0360544221013669

[41] S.-A. Amamra, K. Shi, T. Q. Dinh, and J. Marco, “Optimal day ahead scheduling for plug-in electric vehicles in an industrial microgrid based on v2g system,” in *2019 23rd International Conference on Mechatronics Technology (ICMT)*, 2019, pp. 1–5.

[42] Y.-T. Chai, W.-N. Tan, M.-T. Gan, and S.-C. Yip, “An optimal charging and discharging schedule to maximize revenue for electrical vehicle,” in *2019 IEEE Conference on Sustainable Utilization and Development in Engineering and Technologies (CSUDET)*, 2019, pp. 240–245.

[43] S. Li, J. Li, C. Su, and Q. Yang, “Optimization of bi-directional v2g behavior with active battery anti-aging scheduling,” *IEEE Access*, vol. 8, pp. 11 186–11 196, 2020.

[44] B. Wang, Y. Hu, and F. Zeng, “A user cost and convenience oriented ev charging and discharging scheduling algorithm in v2g based microgrid,” in *2017 International Conference on Circuits, Devices and Systems (ICCDS)*, 2017, pp. 156–162.

[45] X. Chen, K.-C. Leung, A. Y. S. Lam, and D. J. Hill, “Online scheduling for hierarchical vehicle-to-grid system: Design, formulation, and algorithm,” *IEEE Transactions on Vehicular Technology*, vol. 68, no. 2, pp. 1302–1317, 2019.

[46] H. Han, D. Huang, D. Liu, and Q. Li, “Autonomous frequency regulation control of v2g(vehicle-to-grid) system,” in *2017 29th Chinese Control And Decision Conference (CCDC)*, 2017, pp. 5826–5829.

[47] H. Ko, S. Pack, and V. C. M. Leung, “Mobility-aware vehicle-to-grid control algorithm in microgrids,” *IEEE Transactions on Intelligent Transportation Systems*, vol. 19, no. 7, pp. 2165–2174, 2018.

[48] K. D. Afentoulis, Z. N. Bampos, S. I. Vagropoulos, S. D. Keranidis, and P. N. Biskas, “Smart charging business model framework for electric vehicle aggregators,” *Applied Energy*, vol. 328, p. 120179, 2022. [Online]. Available: https://www.sciencedirect.com/science/article/pii/S0306261922014362

[49] İbrahim Şengör, A. Çiçek, A. Kübra Erenoğlu, O. Erdinç, and J. P. Catalão, “User-comfort oriented optimal bidding strategy of an electric vehicle aggregator in day-ahead and reserve markets,” *International Journal of Electrical Power Energy Systems*, vol. 122, p. 106194, 2020. [Online]. Available: https://www.sciencedirect.com/science/article/pii/S0142061519335653

[50] S. Sun, N. Shang, W. Lin, X. Zhou, M. Chen, Z. Rao, Z. Yang, and W. Meng, “A scheduling strategy of vehicle-2-grid based on stackelberg gaming model,” in *2021 IEEE 5th Conference on Energy Internet and Energy System Integration (EI2)*, 2021, pp. 1850–1853.

[51] T. Sousa, “Vehicle-to-grid integration for optimal resource scheduling in the smart grid context,” 2017.

[52] D. Yan, C. Ma, and Y. Chen, “Distributed coordination of charging stations considering aggregate ev power flexibility,” *IEEE Transactions on Sustainable Energy*, vol. 14, no. 1, pp. 356–370, 2023.

[53] L. Wang, J. Kwon, N. Schulz, and Z. Zhou, "Evaluation of aggregated ev flexibility with tso-dso coordination," *IEEE Transactions on Sustainable Energy*, vol. 13, no. 4, pp. 2304–2315, 2022.

[54] M. A. Hannan, M. M. Hoque, A. Hussain, Y. Yusof, and P. J. Ker, "State-of-the-art and energy management system of lithium-ion batteries in electric vehicle applications: Issues and recommendations," *IEEE Access*, vol. 6, pp. 19 362–19 378, 2018.

[55] J. Kronqvist, D. E. Bernal, A. Lundell, and I. E. Grossmann, "A review and comparison of solvers for convex minlp," *Optimization and Engineering*, vol. 20, pp. 397–455, 2019.

[56] C. L. B. Silveira, A. Tabares, L. T. Faria, and J. F. Franco, "Mathematical optimization versus metaheuristic techniques: A performance comparison for reconfiguration of distribution systems," *Electric Power Systems Research*, vol. 196, p. 107272, 2021. [Online]. Available: https://www.sciencedirect.com/science/article/pii/S0378779621002534

[57] R. Allan, R. Billinton, I. Sjarief, L. Goel, and K. So, "A reliability test system for educational purposes-basic distribution system data and results," *IEEE Transactions on Power Systems*, vol. 6, no. 2, pp. 813–820, 1991.

[58] ECF, "Roadmap 2050 - a practical guide to a prosperous, low-carbon europe," 2010.

[59] P. Pinson, H. Madsen, H. A. Nielsen, G. Papaefthymiou, and B. Klöckl, "From probabilistic forecasts to statistical scenarios of short-term wind power production," *Wind Energy*, vol. 12, no. 1, pp. 51–62, 2009. [Online]. Available: https://onlinelibrary.wiley.com/doi/abs/10.1002/we.284

[60] P. Benalcazar, "Optimal sizing of thermal energy storage systems for chp plants considering specific investment costs: A case study," *Energy*, vol. 234, p. 121323, 2021. [Online]. Available: https://www.sciencedirect.com/science/article/pii/S0360544221015711

[61] J. Soares, B. Canizes, C. Lobo, Z. Vale, and H. Morais, "Electric vehicle scenario simulator tool for smart grid operators," *Energies*, vol. 5, no. 6, pp. 1881–1899, 2012. [Online]. Available: https://www.mdpi.com/1996-1073/5/6/1881

[62] "Mitsubichi i-miev technical specifications," 2016, (Consulted: August 2023). [Online]. Available: http://www.mitsubishi-motors.com/en/showroom/i-miev/specifications/

[63] "Citroen c-zero technical specifications," 2016, (Consulted: August 2023). [Online]. Available: https://www.citroen.co.uk/citroen-range.html

[64] "Bmw i3 technical specifications," 2016, (Consulted: August 2023). [Online]. Available: https://www.bmw.pt/pt/all-models.html?tl=grp-wdpl-bcom-mix-mn-.-nscf-.-.-

[65] "Nissan leaf technical specifications," 2016, (Consulted: August 2023).

[66] “Renault zoe simply revolutionary,” 2016, (Consulted: August 2023). [Online]. Available: https://www.renault.co.uk/electric-vehicles/zoe.html

[67] A. Ul-Haq, C. Cecati, and E. El-Saadany, “Probabilistic modeling of electric vehicle charging pattern in a residential distribution network,” *Electric Power Systems Research*, vol. 157, pp. 126–133, 2018. [Online]. Available: https://www.sciencedirect.com/science/article/pii/S0378779617304765

[68] “A comparative study of metaheuristics algorithms based on their performance of complex benchmark problems,” vol. 6. [Online]. Available: https://dmame-journal.org/index.php/dmame/article/view/386

Distribution network data

In this analysis, the base values were set for voltage, power, current and impedance, shown in A.1.

Unit of Measure	Base Value
Voltage (U)	11000 V
Power (S)	1000000 VA
Current (I)	121 A
Impedance (Z)	52.48 Ω

Table A.1: Base Values used for Per Unit system

The following table shows the line information of every branch in the network used.

Line	Bus i to j	Distance (km)	R (p.u.)	X (p.u.)	S (MVA)
1	1-2	0.6	0.00159	0.00056	10
2	2-3	0.75	0.00198	0.00070	10
3	2-4	0.8	0.00212	0.00075	10
4	2-5	0.75	0.00198	0.00070	10
5	5-6	0.8	0.00212	0.00075	10
6	5-7	0.6	0.00159	0.00056	10
7	5-8	0.75	0.00198	0.00070	10
8	8-9	0.8	0.00212	0.00070	10
9	8-10	0.75	0.00198	0.00070	10
10	8-11	0.6	0.00159	0.00056	10
11	11-12	0.8	0.00212	0.00075	10
12	1-13	0.75	0.00198	0.00070	10
13	13-14	0.8	0.00212	0.00075	10
14	13-15	0.6	0.00159	0.00056	10
15	15-16	0.8	0.00212	0.00075	10
16	1-17	0.75	0.00198	0.00070	10
17	17-18	0.6	0.00159	0.00056	10
18	17-19	0.8	0.00212	0.00075	10
19	19-20	0.75	0.00198	0.00070	10
20	19-21	0.8	0.00212	0.00070	10
21	19-22	0.6	0.00159	0.00056	10
22	22-23	0.75	0.00198	0.00070	10
23	22-24	0.8	0.00212	0.00075	10
24	22-25	0.75	0.00198	0.00070	10
25	25-26	0.6	0.00159	0.00056	10
26	1-27	0.8	0.00212	0.00070	10
27	27-28	0.75	0.00198	0.00070	10
28	27-29	0.6	0.00159	0.00056	10
29	27-30	0.75	0.00198	0.00070	10
30	30-31	0.6	0.00159	0.00056	10
31	30-32	0.8	0.00212	0.00070	10
32	30-33	0.75	0.00198	0.00070	10
33	33-34	0.8	0.00212	0.00070	10
34	33-35	0.6	0.00159	0.00056	10
35	35-36	0.75	0.00198	0.00070	10
36	35-37	0.8	0.00212	0.00070	10

Table A.2: Branches information

The detailed active power demands of each load at each time step are shown in the following tables. The demand is shown in per unit values, and identified by its ID, relating to the number of the load and the bus where it is located. The sum of every load demand in each period results in the graphic depicted in Figure 5.3, in Chapter 5. The loads have diverse consumption patterns, categorized into five distinct profiles based on usage behavior. These profiles range from domestic consumption to commercial and service-based consumption, each exhibiting unique load characteristics.

Load ID		**Demand(p.u.)**						
Load	**Bus**	**1**	**2**	**3**	**4**	**5**	**6**	**7**
1	3	0.6527	0.5010	0.4458	0.3962	0.3732	0.3806	0.4045
2	4	0.4219	0.4906	0.4121	0.3434	0.2845	0.20606	0.2551
3	6	0.4992	0.4680	0.3432	0.2392	0.1768	0.0884	0.1248
4	7	0.6903	0.5298	0.4715	0.4190	0.3947	0.4025	0.42773
5	9	0.7920	0.8030	0.8470	0.9350	1.0890	1.0560	1.0450
6	10	0.5612	0.4933	0.4299	0.3530	0.3168	0.2987	0.3439
7	12	0.5647	0.4335	0.3857	0.3428	0.3229	0.3293	0.3500
8	14	0.7924	0.9213	0.7740	0.6450	0.5344	0.3870	0.4791
9	16	1.4008	1.2313	1.07321	0.88113	0.7908	0.7456	0.8585
10	18	0.7489	0.7593	0.8009	0.8841	1.0297	0.9985	0.9881
11	20	0.4992	0.4680	0.3432	0.2392	0.1768	0.0884	0.1248
12	21	0.6527	0.5010	0.4458	0.3962	0.3732	0.3804	0.4045
13	23	0.6859	0.6029	0.52553	0.4314	0.3872	0.3650	0.4204
14	24	0.7920	0.8030	0.8470	0.9350	1.0890	1.0560	1.0450
15	26	0.5647	0.4335	0.3857	0.3428	0.3229	0.3293	0.3500
16	28	0.3650	0.4245	0.3566	0.2971	0.2462	0.1783	0.2207
17	29	0.4199	0.3937	0.2887	0.2012	0.1487	0.0743	0.1049
18	31	0.5490	0.4214	0.3750	0.3332	0.3139	0.3201	0.3402
19	32	0.5455	0.4795	0.4179	0.3431	0.3079	0.2903	0.3343
20	34	0.5280	0.4950	0.3630	0.2530	0.1870	0.0935	0.1320
21	36	0.4462	0.5188	0.4358	0.3632	0.3009	0.2179	0.2698
22	37	0.5647	0.4335	0.3857	0.3428	0.3229	0.3293	0.3500

Table A.3: Load demand from period 1 to 7

Load	Bus	8	9	10	11	12	13	14
Load ID		Demand(p.u.)						
1	3	0.4827	0.5654	0.6068	0.6068	0.6086	0.6123	0.6022
2	4	0.3238	0.3827	0.5005	0.6182	0.7163	0.7556	0.7752
3	6	0.2444	0.4993	0.7697	0.8841	1.0298	0.9882	0.9673
4	7	0.5104	0.5979	0.6417	0.6417	0.6436	0.6475	0.6368
5	9	0.9790	0.8580	0.7590	0.6490	0.6050	0.5610	0.5390
6	10	0.4254	0.5341	0.6246	0.6563	0.6744	0.6834	0.6653
7	12	0.4176	0.4892	0.5250	0.5250	0.5266	0.5298	0.5210
8	14	0.6082	0.7187	0.9399	1.1610	1.3453	1.4190	1.4559
9	16	1.0619	1.3331	1.5590	1.6381	1.6833	1.7059	1.6607
10	18	0.9257	0.8113	0.7177	0.6137	0.5721	0.5305	0.5097
11	20	0.2444	0.4993	0.7697	0.8841	1.0298	0.9882	0.9673
12	21	0.4827	0.5654	0.6068	0.6068	0.6086	0.6123	0.6022
13	23	0.5200	0.6528	0.7634	0.8021	0.8242	0.8353	0.8132
14	24	0.9790	0.8580	0.7590	0.6490	0.6050	0.5610	0.5390
15	26	0.4176	0.4892	0.5250	0.5250	0.5266	0.5298	0.5210
16	28	0.2802	0.3311	0.4330	0.5349	0.6198	0.6538	0.6708
17	29	0.2056	0.4200	0.6474	0.7437	0.8662	0.8312	0.8137
18	31	0.4060	0.4756	0.5104	0.5104	0.5119	0.5150	0.5065
19	32	0.4136	0.5192	0.6072	0.6380	0.6556	0.6644	0.6468
20	34	0.2585	0.5280	0.8140	0.9350	1.0890	1.0450	1.0230
21	36	0.3425	0.4047	0.5293	0.6538	0.7576	0.7991	0.8198
22	37	0.4176	0.4892	0.5250	0.5250	0.5266	0.5298	0.5210

Table A.4: Load demand from period 8 to 14

Load ID		Demand(p.u.)						
Load	**Bus**	**15**	**16**	**17**	**18**	**19**	**20**	**21**
1	3	0.5792	0.5727	0.6978	0.9193	1.0756	1.1905	1.1078
2	4	0.7360	0.6771	0.6182	0.7163	0.8047	0.9960	1.0156
3	6	1.0090	1.0090	0.8737	0.7385	0.6865	0.6137	0.5721
4	7	0.6125	0.6057	0.7379	0.9723	1.1375	1.2591	1.1716
5	9	0.5830	0.6270	0.6710	0.6930	0.6490	0.6270	0.6710
6	10	0.6563	0.6653	0.6879	0.8237	0.9414	1.0409	0.9957
7	12	0.5011	0.4956	0.6038	0.7955	0.9307	1.0301	0.9585
8	14	1.3822	1.2716	1.1610	1.3453	1.5112	1.8705	1.9074
9	16	1.6381	1.6607	1.7172	2.0561	2.3498	2.5983	2.4854
10	18	0.5513	0.5929	0.6345	0.6553	0.6137	0.5929	0.6345
11	20	1.0090	1.0090	0.8737	0.7385	0.6865	0.6137	0.5721
12	21	0.5792	0.5727	0.6978	0.9193	1.0756	1.1905	1.1078
13	23	0.8021	0.8132	0.8408	1.0068	1.1506	1.2723	1.2170
14	24	0.5830	0.6270	0.6710	0.6930	0.6490	0.6270	0.6710
15	26	0.5011	0.4956	0.6038	0.7955	0.9307	1.0301	0.9585
16	28	0.6368	0.5858	0.5349	0.6198	0.6962	0.8618	0.8788
17	29	0.8487	0.8487	0.7349	0.6212	0.5774	0.5162	0.4812
18	31	0.4872	0.4818	0.5869	0.7733	0.9047	1.0014	0.9318
19	32	0.6380	0.6468	0.6688	0.8008	0.9151	1.0119	0.9679
20	34	1.0670	1.0670	0.9240	0.7810	0.7260	0.6490	0.6050
21	36	0.7783	0.7161	0.6538	0.7576	0.8510	1.0533	1.0741
22	37	0.5011	0.4956	0.6038	0.7955	0.9307	1.0301	0.9585

Table A.5: Load demand from period 15 to 21

Load ID		Demand(p.u.)		
Load	**Bus**	**22**	**23**	**24**
1	3	1.0572	0.9929	0.8366
2	4	0.8832	0.6869	0.5691
3	6	0.5357	0.5149	0.4993
4	7	1.1181	1.0500	0.8848
5	9	0.7150	0.7535	0.7755
6	10	0.9142	0.8056	0.6879
7	12	0.9148	0.8591	0.7239
8	14	1.6586	1.2900	1.0689
9	16	2.2820	2.0109	1.7172
10	18	0.6761	0.7125	0.7333
11	20	0.5357	0.5149	0.4993
12	21	1.0572	0.9929	0.8366
13	23	1.1174	0.9847	0.8408
14	24	0.7150	0.7535	0.7755
15	26	0.9148	0.8591	0.7239
16	28	0.7642	0.5943	0.4925
17	29	0.4506	0.4331	0.4200
18	31	0.8893	0.8352	0.7037
19	32	0.8887	0.7832	0.6688
20	34	0.5665	0.5445	0.5280
21	36	0.9340	0.7264	0.6019
22	37	0.9148	0.8591	0.7239

Table A.6: Load demand from period 22 to 24

B

Detailed results from the simulations

The following tables present the detailed results obtain in Model 1, where the DSO assumes the total control of the scheduling. First, the results considering V1G are shown in Tables B.1, B.2 and B.3.

	1	2	3	4	5	6	7	8
Ext. Supplier	12413.93	11239.72	9886.26	8761.60	8422.41	8000	8097.65	9073.60
CHP	1500	1500	1500	1500	1500	1500	1500	1500
PV	0	0	0	0	0	0	93.21	559.28
Storage Dch	0	0	0	0	0	0	0	0
Storage Ch	0	0	0	0	0	125	0	0
Load Cut	0	0	0	0	0	0	0	0
Load Red	0	0	0	0	0	0	0	0
EV Ch	8.74	0	127.23	257.26	347.99	679.68	236.63	90.67

Table B.1: Model 1 results considering V1G from period 1 to 8

	9	10	11	12	13	14	15	16
Ext. Supplier	10050.5	10205.63	9135.61	8981.33	8360.39	8275.11	8327.42	8947.79
CHP	1500	1500	1500	1500	1500	1500	1500	1500
PV	1584.64	3542.14	5592.85	6897.85	7550.35	7736.78	7270.71	6338.57
Storage Dch	0	0	0	0	0	0	0	0
Storage Ch	0	0	0	0	15.69	99.01	9.62	0
Load Cut	0	0	0	0	0	0	0	0
Load Red	0	0	0	0	0	0	0	0
EV Ch	0	0	137.56	267.06	322.74	563.05	334.46	163.54

Table B.2: Model 1 results considering V1G from period 9 to 16

	17	18	19	20	21	22	23	24
Ext. Supplier	10761.1	15244.9	18080.9	20000	20000	18751.6	17375.9	15051.9
CHP	1500	1500	1500	1500	1500	1500	1500	1500
PV	4660.71	2516.78	932.14	279.64	0	0	0	0
Storage Dch	0	0	0	382.50	17.07	0	0	0
Storage Ch	0	0	0	0	0	0	0	0
Load Cut	0	0	0	244.9226	175.84	0	0	0
Load Red	0	0	623.81	680.30	658.30	615.09	0	0
EV Ch	0	0	0	0	0	0	0	0

Table B.3: Model 1 results considering V1G from period 17 to 24

When V2G is considered, the results were the ones depicted in Tables B.4, B.5 and B.6.

Period	1	2	3	4	5	6	7	8
Ext. Supplier	12413.9	11239.7	9921.0	8876.3	8588.3	8050.1	8341.9	9270.9
CHP	1500	1500	1500	1500	1500	1500	1500	1500
PV	0	0	0	0	0	0	93.21	559.28
Storage Dch	0	0	0	0	0	0	0	0
Storage Ch	0	0	0	0	0	0	0	0
Load Cut	0	0	0	0	0	0	0	0
Load Red	0	0	0	0	0	0	0	0
EV Ch	8.74	0	161.01	370.01	511.18	853.11	477.78	284.52
EV Dch	0	0	0	0	0	0	0	0

Table B.4: Model 1 results considering V2G from period 1 to 8

Period	9	10	11	12	13	14	15	16
Ext. Supplier	10050.5	10205.6	9406.1	9227.2	8644.6	8558.8	8653.3	9242.6
CHP	1500	1500	1500	1500	1500	1500	1500	1500
PV	1584.64	3542.14	5592.85	6897.85	7550.35	7736.78	7270.71	6338.57
Storage Dch	0	0	0	0	0	0	0	0
Storage Ch	0	0	0	0	0	0	0	0
Load Cut	0	0	0	0	0	0	0	0
Load Red	0	0	0	0	0	0	0	0
EV Ch	0	0	403.06	508.70	618.16	941.78	665.09	453.30
EV Dch	0	0	0	0	0	0	0	0

Table B.5: Model 1 results considering V2G from period 9 to 16

Period	17	18	19	20	21	22	23	24
Ext. Supplier	10761.1	15244.9	18000	19792.9	19371.4	18079.6	17375.9	15052.8
CHP	1500	1500	1500	1500	1500	1500	1500	1500
PV	4660.71	2516.78	932.14	279.64	0	0	0	0
Storage Dch	0	0	0	230.04	9.95	0	0	0
Storage Ch	0	0	0	0	0	0	0	0
Load Cut	0	0	0	0	0	0	0	0
Load Red	0	0	555.31	680.30	658.30	615.09	0	0
EV Ch	0	0	0	0	0	0	0	0.90
EV Dch	0	0	145.62	600.75	789.31	644.43	0	0

Table B.6: Model 1 results considering V2G from period 17 to 24

The following tables depict the results of the DSO scheduling in Model 2. The data presented in the next tables is referred to days 1 through 4, as those were the cases studied more deeply in this study.

Period	1	2	3	4	5	6	7	8
Ext. Supplier	12413.79	11636.29	10053.81	8741.55	8247.67	7403.09	7913.64	9037.89
CHP	1500	1500	1500	1500	1500	1500	1500	1500
PV	0	0	0	0	0	0	93.21	559.28
Storage Dch	0	0	0	0	0	0	0	0
Storage Ch	0	0	0	0	0	125	0	0
Load Cut	0	0	0	0	0	0	0	0
Load Red	0	0	0	0	0	0	0	0
EVA flex	0	0	0	0	0	0	0	0

Table B.7: Model 2 results for day 1-4 from period 1 to 8

Period	9	10	11	12	13	14	15	16
Ext. Supplier	10411.76	10440.76	9148.16	8830.93	8125.17	7937.96	8145.93	9143.50
CHP	1500	1500	1500	1500	1500	1500	1500	1500
PV	1584.64	3542.14	5592.85	6897.85	7550.35	7736.78	7270.71	6338.57
Storage Dch	0	0	0	0	0	0	0	0
Storage Ch	0	0	0	0	0	125	0	0
Load Cut	0	0	0	0	0	0	0	0
Load Red	0	0	0	0	0	0	0	0
EVA flex	0	0	0	0	0	0	0	0

Table B.8: Model 2 results for day 1-4 from period 9 to 16

Period	17	18	19	20	21	22	23	24
Ext. Supplier	11026.31	15471.86	18158.61	20000	20000	18926.12	17506.09	15051.93
CHP	1500	1500	1500	1500	1500	1500	1500	1500
PV	4660.71	2516.78	932.14	279.64	0	0	0	0
Storage Dch	0	0	0	358.21	41.78	0	0	0
Storage Ch	0	0	0	0	0	0	0	0
Load Cut	0	0	0	0	0	0	0	0
Load Red	0	0	623.81	680.30	658.30	615.09	0	0
EVA flex	0	0	0	354.87	327.81	0	0	0

Table B.9: Model 2 results for day 1-4 from period 17 to 24

The following tables represent the DSO power scheduling on days 8 through 10, where no flexibility was used, thus no power curtailment was imposed on the EVAs.

Period	1	2	3	4	5	6	7	8
Ext. Supplier	12413.79	11636.29	10053.81	8741.55	8247.67	7403.09	7913.64	9037.89
CHP	1500	1500	1500	1500	1500	1500	1500	1500
PV	0	0	0	0	0	0	93.21	559.28
Storage Dch	0	0	0	0	0	0	0	0
Storage Ch	0	0	0	0	0	125	0	0
Load Cut	0	0	0	0	0	0	0	0
Load Red	0	0	0	0	0	0	0	0
EVA flex	0	0	0	0	0	0	0	0

Table B.10: Model 2 results for day 8-10 from period 1 to 8

Period	9	10	11	12	13	14	15	16
Ext. Supplier	10411.76	10440.76	9148.16	8830.93	8125.17	7937.96	8145.93	9143.50
CHP	1500	1500	1500	1500	1500	1500	1500	1500
PV	1584.64	3542.14	5592.85	6897.85	7550.35	7736.78	7270.71	6338.57
Storage Dch	0	0	0	0	0	0	0	0
Storage Ch	0	0	0	0	0	125	0	0
Load Cut	0	0	0	0	0	0	0	0
Load Red	0	0	0	0	0	0	0	0
EVA flex	0	0	0	0	0	0	0	0

Table B.11: Model 2 results for day 8-10 from period 9 to 16

Period	17	18	19	20	21	22	23	24
Ext. Supplier	11026.31	15471.86	18158.61	20000	20000	18926.12	17506.09	15051.93
CHP	1500	1500	1500	1500	1500	1500	1500	1500
PV	4660.71	2516.78	932.14	279.6429	0	0	0	0
Storage Dch	0	0	0	333.96	66.03	0	0	0
Storage Ch	0	0	0	0	0	0	0	0
Load Cut	0	0	0	370.13	295.85	0	0	0
Load Red	0	0	623.81	680.47	658.30	615.09	0	0
EVA flex	0	0	0	0	0	0	0	0

Table B.12: Model 2 results for day 8-10 from period 17 to 24